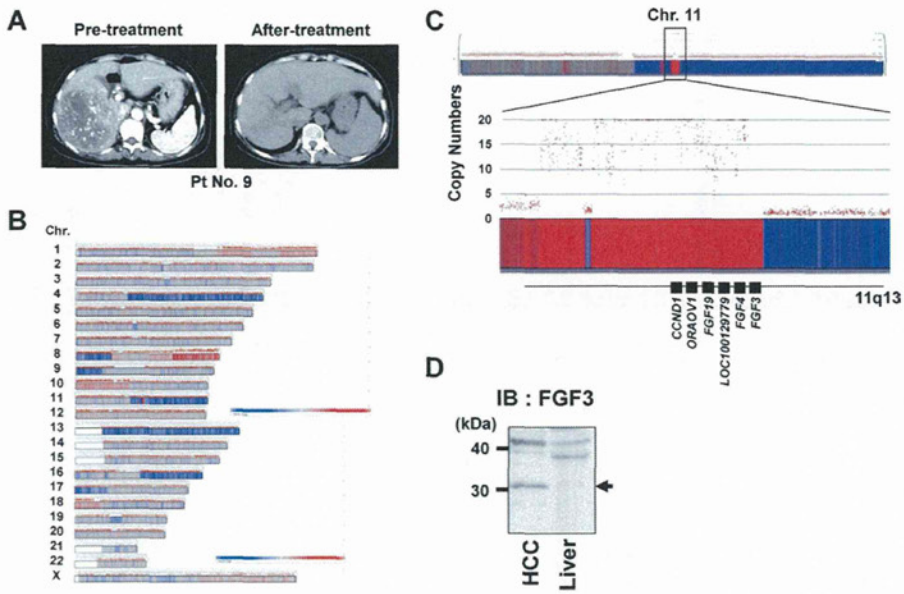

Fig. 1. HCC exhibiting a marked response to sorafenib treatment harbors *FGF3/FGF4* gene amplification. (A) Abdominal CT images obtained pretreatment (left panel) and 2 months after treatment (right panel). (B) CGH analysis of the tumor. Paired background liver tissue was used as a reference sample. A gain (>4 copies, red) and a loss (<0.5 copies, blue) of genomic copy number are shown. (C) Whole copy numbers of chromosome 11 are shown. A highly amplified region is described in the lower panel. (D) Western blot analysis of FGF3 (arrow) in HCC and paired background liver samples. IB, immunoblotting.

GGA GGG TCA CAG CCT GGG GAG GAA GTG GGT GAC CTT C-3′ (reverse). The stable transfectants expressing *EGFP* or *FGF3* or *FGF4* for each cell line were designated as A549/EGFP, A549/FGF3, and A549/FGF4.

Xenograft Studies. Nude mice (BALB/c nu/nu, 6-week-old females; CLEA Japan Inc., Tokyo) were used for *in vivo* studies and were cared for in accordance with the recommendations for the handling of laboratory animals for biomedical research compiled by the Committee on Safety and Ethical Handling Regulations for Laboratory Animal Experiments, Kinki University. Mice were subcutaneously inoculated with a total of 5×10^6 A549/EGFP, A549/FGF3, or A549/FGF4 cells. Two weeks after inoculation, the mice were randomized according to tumor size into two groups to equalize the mean pretreatment tumor size among the three groups (n = 20 mice per group). The mice were then treated with a low dose of oral sorafenib (n = 10, 15 mg/kg/day) or vehicle control (n = 10, Cremophor EL/ethanol/water) for 9 days. Tumor volume was calculated as length × width^2 × 0.5 and was assessed every 2 to 3 days.

Statistical Analysis. The statistical analyses were performed to test for differences between groups using the Student *t* test or Fisher's exact test. $P < 0.05$ was considered statistically significant. All analyses were performed using PAWS Statistics 18 (SPSS Japan Inc., Tokyo, Japan).

Results

Responder to Sorafenib Who Harbored* FGF3/FGF4 *Gene Amplification. A 58-year-old woman was diagnosed as having histologically confirmed advanced HCC (Fig. 1A, left panel) with multiple lung metastases. She received combination treatment with sorafenib, 5-fluorouracil (5FU), and interferon, and a subsequent treatment assessment revealed a partial response. Because the disease was well controlled with sorafenib treatment for 14 months (Fig. 1A, right panel), surgery was performed. To characterize this tumor molecularly, we performed array CGH analysis using frozen surgical specimens of the HCC region and paired background liver tissue as a reference control. The array CGH analysis revealed a low-level gain in the genomic DNA copy number for 1q, 8q, 10p, and 18p and a high level gain at 11q13 (Fig. 1B). Interestingly, the 11q13 region, a rare amplicons in HCC that contains several genes, including *FGF3*, *FGF4*, *CCND1*, and *FGF19*, was highly amplified over 20 copies (Fig. 1C). Western blot analysis revealed that FGF3 was overexpressed in the HCC specimen compared with the paired background liver specimen (Fig. 1D).

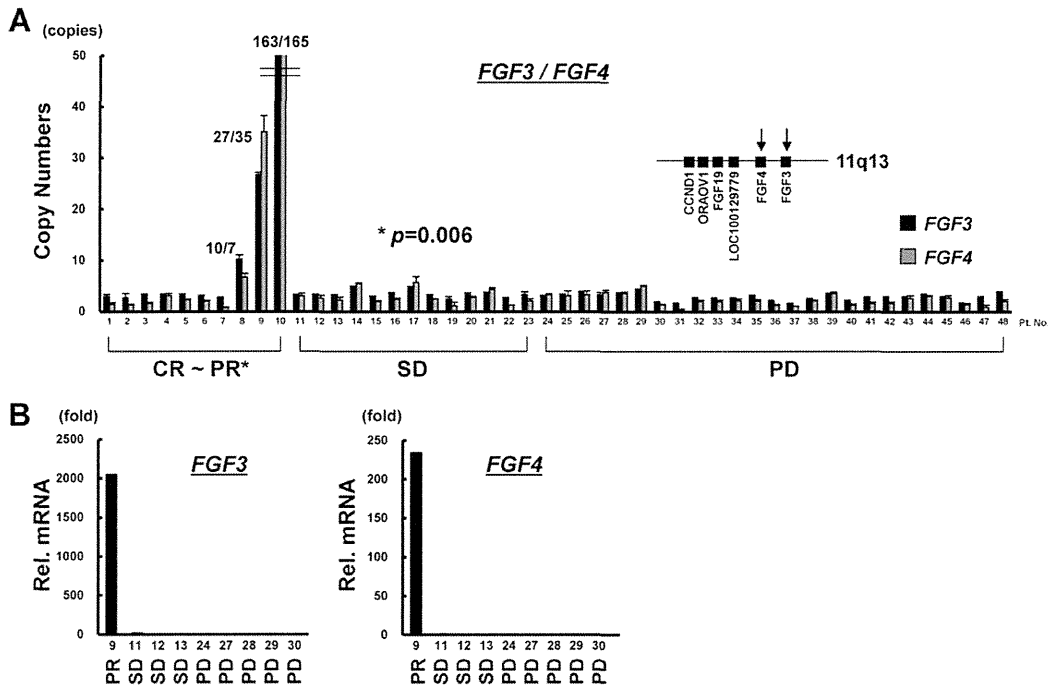

Fig. 2. *FGF3/FGF4* gene amplification is frequently observed in responders to sorafenib in HCC. (A) *FGF3/FGF4* gene amplification was determined using the TaqMan copy number assay in DNA samples obtained from 48 HCC samples that had been treated with sorafenib. *FGF3* amplification of >5 copies was observed in three of the sorafenib responders. *Complete response + partial response versus stable disease + progressive disease. (B) *FGF3/FGF4* gene amplification mediates the overexpression of *FGF3/FGF4* mRNA. The mRNA expression levels of *FGF3* and *FGF4* were examined in nine HCC samples that were available as frozen samples among 48 HCC samples that were treated with sorafenib. Rel. mRNA, *target gene/GAPD* $\times$ 10^6.

The 11q13 locus is known to be a frequently amplified region in several human cancers except HCC.[13] Thus, we hypothesized that the amplification of 11q13 may be involved in a marked response to sorafenib.

FGF3/FGF4 ***Gene Amplification Is Frequently Observed in Responders to Sorafenib.*** To address the question of whether *FGF3/FGF4* gene amplification is also found in the HCC of other responders to sorafenib, we examined HCC specimens collected from 11 other medical centers in Japan. Because most of the HCC samples were collected as FFPE samples, we used a TaqMan Copy number assay.[10] A copy number assay revealed that *FGF3/FGF4* amplification was observed in three of the 10 (30%) HCC samples that responded to sorafenib, whereas no amplification was observed in the 38 specimens from patients with stable or progressive disease (P = 0.006, Fig. 2A). The copy numbers for *FGF3/FGF4* were 10.2 $\pm$ 0.8/6.7 $\pm$ 0.8, 26.7 $\pm$ 0.4/35.1 $\pm$ 3.1, and 162.5 $\pm$ 9.0/165.0 $\pm$ 12.5 copies in the amplified samples, whereas the copy numbers of *FGF3* for all the other samples were below 5 copies. The correlation between the *FGF3* locus and the *FGF4* locus copy numbers was very high (R = 0.998), indicating that the DNA copy number assay for *FGF3/FGF4* was a sensitive and reproducible method.

FGF3/FGF4 ***Gene Amplification Mediates the Overexpression of*** **FGF3/FGF4** ***Messenger RNA.*** We examined the messenger RNA (mRNA) expression levels of *FGF3/FGF4* in nine HCC samples that were available as frozen samples among the 48 sorafenib-treated samples, as shown in Fig. 2A. One amplified sample expressed extremely high mRNA levels of *FGF3/FGF4* compared with nonamplified samples (Fig. 2B). The results demonstrated that *FGF3/FGF4* gene amplification mediates the overexpression of *FGF3/FGF4* mRNAs and proteins (Figs. 2B and 1D).

FISH Analysis Confirmed **FGF3/FGF4** ***Gene Amplification.*** We used FISH analysis to examine *FGF3/FGF4* amplification and to verify the results of the above-described PCR-based DNA copy number assay. All *FGF3/FGF4*-amplified clinical samples were confirmed as exhibiting high-level *FGF3* amplification using FISH analysis (Fig. 3). One patient showed multiple scattered signals, whereas two patients showed large clustered signals. Nonamplified HCC yielded a negative result for gene amplification. These results clearly demonstrate the presence of *FGF3/FGF4*-

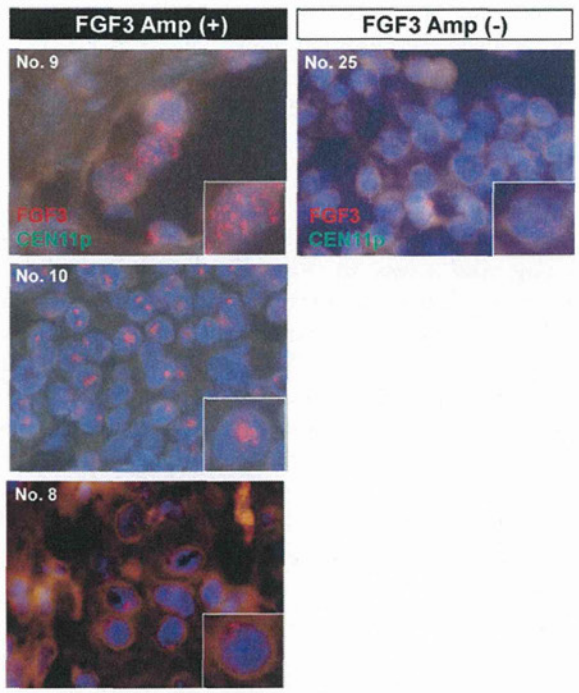

Fig. 3. FISH analysis of *FGF3*-amplified HCC. Patient numbers were indicated. Green staining indicates *CEN11P* loci; red staining indicates *FGF3* loci. High-power images are presented in each inset for a single cancer cell. Amp, gene amplification.

amplified HCC among the clinical samples, and the FISH analysis results were consistent with those for the copy number assay.

Frequency of* FGF3/FGF4 *Gene Amplification in HCC. To determine the frequency of *FGF3/FGF4* gene amplification in HCC, we performed a copy number assay for HCC samples without sorafenib treatment in a series of surgical specimens. Two of the 82 (2.4%) HCC samples exhibited *FGF3/FGF4* gene amplification, with copy numbers of 10.7/15.3 and 133.3/112.7 copies, respectively (Fig. 4). One amplified HCC was a poorly differentiated tumor, whereas the other was a moderately differentiated tumor.

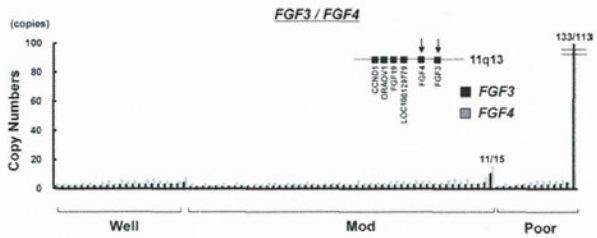

Fig. 4. *FGF3/FGF4* gene amplification in a series of HCC samples without sorafenib treatment. TaqMan copy number assay for *FGF3* and *FGF4* was used to examine DNA samples obtained from 82 surgical specimens. Human normal genomic DNA was used as a normal control. Well, well-differentiated HCC; Mod, moderately differentiated HCC; Poor, poorly differentiated HCC.

Clinicopathological Features of Responders to Sorafenib. The clinico-pathological features of the sorafenib responders are shown in Table 1. A comparison of clinical factors (age, sex, viral status, alpha-fetoprotein level, PIVKA-II, clinical stage, primary tumor size, metastatic status, histological type, and tumor response between responders and nonresponders) is given in Table 2. Notably, multiple lung metastases over five nodules was significantly higher among responders to sorafenib (responders, 5/13 [38%]; nonresponders, 2/42 [5%]; $P = 0.006$). Although the difference was not significant, poorly differentiated HCC tended to be

Table 1. Clinico-pathological Characteristics in Sorafenib Responders

Patient No.	Age, Years	Sex	Viral Status	AFP, ng/mL	PIVKA-II, mAU/mL	Clinical Stage	HCC in the Liver	Lung Metastasis	Other Metastases	Histological Type	Combination Treatment	Treatment Response	*FGF3/FGF4* Amplification
1	52	M	B	198	140	IV	2 cm, ×3	multi	Adrenal gland	Mod	(−)	PR	(−)
2	63	M	B	24	1,983	III	6 cm	(−)	(−)	Mod	(−)	CR	(−)
3	58	M	C	16	14	III	9 cm, multiple	(−)	(−)	Well	(−)	PR	(−)
4	62	M	B	8	130	IV	(−)	×3	(−)	Mod-Poor	(−)	PR	(−)
5	47	F	C	1,872	728	IV	2 cm, multiple	Multiple	(−)	Poor	+TAI	CR	(−)
6	66	M	C	290	18,507*	IV	5 cm	(−)	(−)	Mod	(−)	CR	(−)
7	71	M	C	404,100	1,328	IV	5 cm, multiple	Multiple	(−)	Poor	(−)	CR	(−)
8	66	M	Non	49	7,173	IV	(−)	×2	Pleural, LN	Mod	(−)	PR	Amplification
9	58	F	B	715	101	IV	11 cm	Multiple	(−)	Combination†	+5FU/IFN	PR	Amplification
10	80	F	C	378	21	III	3 cm, ×3	(−)	(−)	Poor, Mod‡	(−)	CR	Amplification
11	57	M	C	46,835	2,730	IV	14 cm, multiple	Multiple	(−)	Mod	(−)	CR	ND
12	77	M	B	435	71,000	IV	4 cm, multiple	(−)	(−)	Mod	(−)	PR	ND
13	84	M	Non	5,410	847,000*	IV	13 cm, multiple	(−)	(−)	Poor	(−)	PR	ND

Abbreviations: AFP, alpha-fetoprotein; CR, complete response; F, female; IFN, interferon; LN, lymph node; M, male; Mod, moderately differentiated; ND, not done; Non, non-B, non-C; Poor, poorly differentiated; PR, partial response; TAI, transcatheter arterial infusion; Well, well differentiated.

*Warfarin treatment (+).

†HCC with cholangiocarcinoma component.

‡From two different HCC nodules.

Table 2. Clinicopathological Characteristics and *FGF3/FGF4* Gene Amplification in Responders and Nonresponders to Sorafenib

Characteristic	Responders (n = 13)	Nonresponders (n = 42)	*P* Value*
Age, years (range)	63 (47-84)	66 (22-89)	0.98
Sex, M/F	10/3	30/12	0.97
Viral status, no.			0.69
HBV	5	10	
HCV	6	16	
B+C	0	1	
Non-B, non-C	2	15	
AFP, ng/mL (range)	378 (8-404,100)	56 (2-114,248)	0.33
PIVKA-II, mAU/mL (range)	728 (14-847,000)	81 (11-147,000)	0.78
Clinical stage, no.			0.73
II	0	1	
III	3	13	
IV	10	28	
Primary tumor, cm (range)	5 (0-14)	3 (0-15)	0.20
Lung metastasis, no.			0.13
(−)	6	31	
(+)	7	11	
Multiple lung metastases, no.			0.006
<5	8	40	
≥5	5	2	
Other metastases, no.			0.24
(−)	11	26	
(+)	2	16	
Histological type, no.			0.13
Well	1	7	
Moderate	6	26	
Poor	5	6	
Combination†	1	3	
Response, no.			ND
Complete response	6	–	
Partial response	7	–	
Stable disease	–	16	
Progressive disease	–	24	
Not evaluable	–	2	

Abbreviations: AFP, alpha-fetoprotein; HBV, hepatitis B virus; HCV, hepatitis C virus; ND, not done.

*P values of viral status and histological type were calculated between HBV versus HCV and poorly differentiated versus nonpoorly differentiated.

†HCC with cholangiocarcinoma component.

more common among responders to sorafenib (responders, 5/13 [38%]; nonresponders, 6/42 [14%]; $P = 0.13$). These results suggest that multiple lung metastases and a poorly differentiated histology may be clinical biomarkers for sorafenib treatment in patients with HCC.

Sorafenib Potently Inhibits Cellular Growth in* FGF3/FGF4-*Amplified and* FGFR2-*Amplified Cell Lines. We examined the growth inhibitory effect of sorafenib in various cancer cell lines to evaluate whether activated FGFR signaling is involved in the response to sorafenib. Among 26 cell lines, KYSE220 was the only *FGF3/FGF4*-amplified cell line (data not shown), and HSC-43, HSC-39, and KATOIII were the only *FGFR2*-amplified cell lines.[14] Sorafenib potently inhibited cellular growth in these four cell lines at a sub-μM 50% inhibitory concentration (IC_{50}) (Fig. 5A). The IC_{50} values were as follows: HSC43, 0.8 μM; HSC39, 0.6 μM; KATOIII, 0.4 μM; and KYSE220, 0.18 μM. These results suggest that activated FGFR signaling may be involved in the response to sorafenib.

***Sorafenib Inhibits Tumor Growth in* FGF4-*Introducing Cell Lines* In Vivo.** Finally, we established cancer cell lines stably overexpressing *EGFP*, *FGF3*, or *FGF4* to examine the relationship between the gene function of *FGF3* or *FGF4* and drug sensitivity to sorafenib *in vivo*. Western blotting confirmed that exogenously expressed FGF3 and FGF4 were secreted into the culture medium (Fig. 5B). Sorafenib inhibited the FGF4-conditioned, medium-mediated expression levels of phosphorylated FGFR (Figure 5C). A similar result was obtained using recombinant FGF4 (data not shown). Mice inoculated with these cell lines were treated with a low dose of oral sorafenib (15 mg/kg/day) or without sorafenib (vehicle control). *FGF3* overexpression did not increase the tumor volume compared with EGFP tumors; however, *FGF4* overexpression aggressively increased tumor volume and clearly enhanced the malignant phenotype (Fig. 5D). Notably, the low-dose sorafenib treatment significantly inhibited the growth of the A549/FGF4 tumors, whereas it was not effective against A549/EGFP and A549/FGF3 tumors (Fig. 5D). These results suggest that overexpression of *FGF4* is partially involved in the response to sorafenib.

Discussion

The *FGF3* gene was first identified and characterized based on its similarity to the mouse *fgf3/int-2* gene, which is a proto-oncogene activated in virally induced mammary tumors in mice.[15] Meanwhile, the *FGF4* gene was first identified in gastric cancer as an oncogene *HST*, which has the ability to induce the neoplastic transformation of NIH-3T3 cells upon transfection.[16] These genes were initially regarded as proto-oncogenes. *FGF3* and *FGF4* genes are located side-by-side and are also closely located to the *FGF19* and *CCND1* genes (within 0.2 Mb of the 11q13 region).[13] The 11q13 region is known as a gene-dense region, and gene amplification of this region is frequently observed in various solid cancers (including breast cancer, squamous cell carcinoma of the head and neck, esophageal cancer, and melanoma) at frequencies of 13%-60%.[13] On the other hand, the frequency of *FGF3/FGF4* amplification in HCC remains

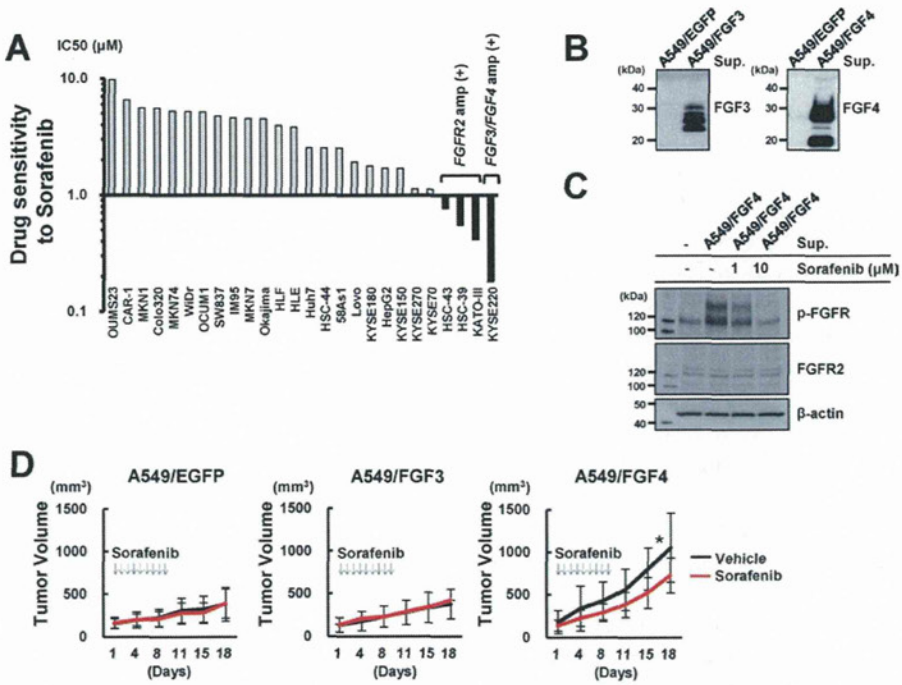

Fig. 5. FGF3 and FGF4 overexpression and drug sensitivity to sorafenib *in vitro* and *in vivo*. (A) Growth inhibitory assay examining sorafenib in various cancer cell lines *in vitro*. The growth inhibitory effect of sorafenib was examined using an MTT assay. The IC_{50} values of each cell line are shown in the graph. The black bars show that the IC_{50} values were below 1 μM. Amp, gene amplification. (B) Cancer cell lines stably overexpressing *EGFP*, *FGF3*, or *FGF4* were established and designated as A549/EGFP, A549/FGF3, and A549/FGF4. Western blot analysis confirmed that exogenously expressed FGF3 and FGF4 were secreted into the culture medium. Sup., supernatant. (C) NIH-3T3 cells were exposed to indicated concentrations of sorafenib for 2 hours and were then stimulated with FGF4-conditioned medium for 20 minutes. (D) Mice inoculated with A549/EGFP, A549/FGF3, or A549/FGF4 (n = 20 each) were treated with a low dose of oral sorafenib (n = 10, 15 mg/kg/day) or without (n = 10, vehicle control). $^*P < 0.05$.

largely unclear. Relatively small cohort studies have reported that one out of 20 HCCs exhibited *FGF3* amplification as determined via CGH analysis,[17] and 3 out of 45 HCCs examined using Southern blot analysis had a copy number >5;[18] meanwhile, amplification was not detected in 0 out of 42 surgically resected HCCs.[19] In the present study, two of the 82 (2.4%) HCC samples exhibited *FGF3/FGF4* gene amplification in the HCC series. If only 2%-3% of HCC patients harbor the *FGF3/FGF4* amplification, its value as a biomarker seems to be limited in clinics because a frequency of 2%-3% is too low to stratify the patients for specific targeted therapy. However, a combination of biomarkers—including *FGF3/FGF4* amplification, lung metastasis, tumor differentiation, and other unrevealed dysregulation of FGFR signaling—may increase the response prediction. In addition, 2%-3% of *FGF3/FGF4* amplification may be a promising therapeutic target for future FGFR-targeted therapies in the treatment of HCC.

Tumor shrinkage might be due to the mixed effect (sorafenib + 5FU + interferon) of combination therapy in the initially described patient. However, during this patient's long clinical course, tumor regrowth was observed following withdrawal of sorafenib because of oral hemorrhage, and tumor reshrinkage was observed when sorafenib treatment recommenced. Thus, we considered that tumor shrinkage might be achieved by the effect of sorafenib on its own, rather than 5FU + interferon.

Regarding determinants of drug sensitivity to sorafenib, the mechanism of hypersensitivity in the gastric cancer cell lines HSC-39, HSC-43, and KATO-III is *FGFR2* gene amplification and is thought to be the addiction of these cell lines to this gene,[14] since sorafenib has a relatively weak but significant inhibitory effect on FGFR1 at a concentration of 580 ± 100 nM.[3] This result suggests that the blockade of FGFR signaling by sorafenib may lead to a significant treatment response, at least in *FGFR2*-amplified cells. In this study, we found that *FGF4*, but not *FGF3* overexpression, was partially involved in the sensitivity to sorafenib *in vivo*. The limitations of the study are the small number of responder patients and the potential bias in their selection because of the retrospective study design. Further clinical study of responders to

sorafenib is necessary. We are presently undertaking a prospective molecular translational study (2010-2012) in a cohort of Japanese patients with sorafenib-treated HCC.

Multiple lung metastases were frequently observed among responders to sorafenib (38%) but were less common among nonresponders (5%). Based on a Japanese follow-up survey of patients with primary HCC, lung metastasis was observed in 7% (169/2355) of the patients at the time of autopsy.[20] Another study demonstrated that 15% of patients were found to have extrahepatic metastases, and lung metastasis was detected in 6% of 995 consecutive HCC patients.[21] When compared with these data from large-scale studies, the frequency of lung metastasis among responders to sorafenib seems quite high. In addition, a poorly differentiated histological type tended to be more common among responders, although the correlation was not significant.

In conclusion, we found that *FGF3/FGF4* gene amplification, multiple lung metastases, and a poorly differentiated histological type may be involved in the response to sorafenib.

References

1. Jemal A, Murray T, Ward E, Samuels A, Tiwari RC, Ghafoor A, et al. Cancer statistics, 2005. Ca Cancer J Clin 2005;55:10-30.
2. Yamamoto J, Kosuge T, Takayama T, Shimada K, Yamasaki S, Ozaki H, et al. Recurrence of hepatocellular carcinoma after surgery. Br J Surg 1996;83:1219-1222.
3. Wilhelm SM, Carter C, Tang L, Wilkie D, McNabola A, Rong H, et al. BAY 43–9006 exhibits broad spectrum oral antitumor activity and targets the RAF/MEK/ERK pathway and receptor tyrosine kinases involved in tumor progression and angiogenesis. Cancer Res 2004;64:7099-7109.
4. Llovet JM, Ricci S, Mazzaferro V, Hilgard P, Gane E, Blanc JF, et al. SHARP Investigators Study Group. Sorafenib in advanced hepatocellular carcinoma. N Engl J Med 2008;359:378-390.
5. Cheng AL, Kang YK, Chen Z, Tsao CJ, Qin S, Kim JS, et al. Efficacy and safety of sorafenib in patients in the Asia-Pacific region with advanced hepatocellular carcinoma: a phase III randomised, double-blind, placebo-controlled trial. Lancet Oncol 2009;10:25-34.
6. So BJ, Bekaii-Saab T, Bloomston MA, Patel T. Complete clinical response of metastatic hepatocellular carcinoma to sorafenib in a patient with hemochromatosis: a case report. J Hematol Oncol 2008;1:18.
7. Nakazawa T, Hidaka H, Shibuya A, Koizumi W. Rapid regression of advanced hepatocellular carcinoma associated with elevation of des-gamma-carboxyprothrombin after short-term treatment with sorafenib—a report of two cases. Case Rep Oncol 2010;3:298-303.
8. Paez JG, Janne PA, Lee JC, Tracy S, Greulich H, Gabriel S, et al. EGFR mutations in lung cancer: correlation with clinical response to gefitinib therapy. Science 2004;304:1497-1500.
9. Lynch TJ, Bell DW, Sordella R, Gurubhagavatula S, Okimoto RA, Brannigan BW, et al. Activating mutations in the epidermal growth factor receptor underlying responsiveness of non-small-cell lung cancer to gefitinib. N Engl J Med 2004;350:2129-2139.
10. Matsumoto K, Arao T, Hamaguchi T, Shimada Y, Kato K, Oda I, et al. FGFR2 gene amplification and clinicopathological features in gastric cancer. Br J Cancer 2012;14:727-732.
11. Matsumoto K, Arao T, Tanaka K, Kaneda H, Kudo K, Fujita Y, et al. mTOR signal and hypoxia-inducible factor-1 alpha regulate CD133 expression in cancer cells. Cancer Res 2009;69:7160-7164.
12. Kaneda H, Arao T, Tanaka K, Tamura D, Aomatsu K, Kudo K, et al. FOXQ1 is overexpressed in colorectal cancer and enhances tumorigenicity and tumor growth. Cancer Res 2010;70:2053-2063.
13. Ormandy CJ, Musgrove EA, Hui R, Daly RJ, Sutherland RL. Cyclin D1, EMS1 and 11q13 amplification in breast cancer. Breast Cancer Res Treat 2003;78:323-335.
14. Takeda M, Arao T, Yokote H, Komatsu T, Yanagihara K, Sasaki H, et al. AZD2171 shows potent antitumor activity against gastric cancer over-expressing fibroblast growth factor receptor 2/keratinocyte growth factor receptor. Clin Cancer Res 2007;13:3051-3057.
15. Peters G, Brookes S, Smith R, Dickson C. Tumorigenesis by mouse mammary tumor virus: evidence for a common region for provirus integration in mammary tumors. Cell 1983;33:369-377.
16. Sakamoto H, Mori M, Taira M, Yoshida T, Matsukawa S, Shimizu K, et al. Transforming gene from human stomach cancers and a noncancerous portion of stomach mucosa. Proc Natl Acad Sci U S A 1986;83:3997-4001.
17. Takeo S, Arai H, Kusano N, Harada T, Furuya T, Kawauchi S, et al. Examination of oncogene amplification by genomic DNA microarray in hepatocellular carcinomas: comparison with comparative genomic hybridization analysis. Cancer Genet Cytogenet 2001;130:127-132.
18. Nishida N, Fukuda Y, Komeda T, Kita R, Sando T, Furukawa M, et al. Amplification and overexpression of the cyclin D1 gene in aggressive human hepatocellular carcinoma. Cancer Res 1994;54:3107-3110.
19. Chochi Y, Kawauchi S, Nakao M, Furuya T, Hashimoto K, Oga A, et al. A copy number gain of the 6p arm is linked with advanced hepatocellular carcinoma: an array-based comparative genomic hybridization study. J Pathol 2009;217:677-684.
20. Ikai I, Arii S, Ichida T, Okita K, Omata M, Kojiro M, et al. Report of the 16th follow-up survey of primary liver cancer. Hepatol Res 2005;32:163-172.
21. Uka K, Aikata H, Takaki S, Shirakawa H, Jeong SC, Yamashina K, et al. Clinical features and prognosis of patients with extrahepatic metastases from hepatocellular carcinoma. World J Gastroenterol 2007;13:414-420.

Cancer Science
The official journal of the Japanese Cancer Association

Clinical phase I study of elpamotide, a peptide vaccine for vascular endothelial growth factor receptor 2, in patients with advanced solid tumors

Isamu Okamoto,[1] Tokuzo Arao,[2] Masaki Miyazaki,[1] Taroh Satoh,[1] Kunio Okamoto,[1] Takuya Tsunoda,[3] Kazuto Nishio[2,4] and Kazuhiko Nakagawa[1]

Departments of [1]Medical Oncology and [2]Genome Biology, Kinki University Faculty of Medicine, Osaka; [3]OncoTherapy Science, Kawasaki, Japan

(Received July 19, 2012/Revised August 22, 2012/Accepted August 28, 2012/Accepted manuscript online September 7, 2012/Article first published online October 14, 2012)

Targeting of tumor angiogenesis with vaccines is a potentially valuable approach to cancer treatment. Elpamotide is an immunogenic peptide derived from vascular endothelial growth factor receptor 2, which is expressed at a high level in vascular endothelial cells. We have now carried out a phase I study to evaluate safety, the maximum tolerated dose, and potential pharmacodynamic biomarkers for this vaccine. Ten HLA-A*24:02-positive patients with advanced refractory solid tumors received elpamotide s.c. at dose levels of 0.5, 1.0, or 2.0 mg once a week on a 28-day cycle. Five patients experienced an injection site reaction of grade 1 and 2, which was the most frequent adverse event. In the 1.0 mg cohort, one patient experienced proteinuria of grade 1 and another patient developed both hypertension and proteinuria of grade 1. No adverse events of grade 3 or higher were observed, and the maximum tolerated dose was therefore not achieved. The serum concentration of soluble vascular endothelial growth factor receptor 2 decreased significantly after elpamotide vaccination. Microarray analysis of gene expression in PBMCs indicated that several pathways related to T cell function and angiogenesis were affected by elpamotide vaccination, supporting the notion that this peptide induces an immune response that targets angiogenesis in the clinical setting. In conclusion, elpamotide is well tolerated and our biomarker analysis indicates that this anti-angiogenic vaccine is biologically active. Clinical trial registration no. UMIN000008336. (*Cancer Sci* 2012; 103: 2135–2138)

Angiogenesis, defined as the formation of new blood vessels from pre-existing vasculature, is essential for tumor growth and the spread of metastases.[1,2] Vascular endothelial growth factor (VEGF) is a pro-angiogenic molecule that plays a central role in angiogenesis, primarily through activation of VEGF receptor 2 (VEGFR2). Several approaches to the targeting of VEGF–VEGFR pathways, including those based on neutralizing antibodies to VEGF, small-molecule VEGFR tyrosine kinase inhibitors, and soluble VEGFR constructs (VEGF-Trap), are emerging as promising therapeutic options in clinical oncology.[3]

Vascular endothelial growth factor 2 has been a major target for anti-angiogenic therapy to date. Studies in mice have shown that tumor angiogenesis is inhibited as a result of cellular immune responses induced by vaccination with cDNA encoding mouse VEGFR2 or with a soluble fragment of the receptor.[4,5] On the basis of these findings, we have examined the possibility of developing a novel anti-angiogenic immunotherapy for cancer in the clinical setting. We previously identified peptide epitopes of human VEGFR2 and showed that CTLs induced by these peptides manifest potent and specific HLA class I-restricted cytotoxicity toward not only peptide-pulsed target cells but also endothelial cells expressing endogenous VEGFR2.[6] Furthermore, vaccination with peptides corresponding to these epitopes inhibited angiogenesis induced by tumor xenografts, resulting in marked suppression of tumor growth and prolongation of animal survival without the occurrence of fatal adverse events.[6]

We have now carried out a phase I clinical trial for treatment of HLA-A*24:02-positive patients with advanced refractory solid tumors by vaccination with the VEGFR2-169 peptide (elpamotide), which was previously shown to be the most effective among human VEGFR2 epitopic peptides tested for the ability to induce CTL precursors among PBMCs from cancer patients.[7] We examined the safety of this treatment as a primary endpoint, and the clinical and biological responses as secondary endpoints.

Patients and Methods

Patient eligibility. HLA-A*24:02-positive individuals aged ≥ 20 years with a histologically confirmed diagnosis of an advanced tumor refractory to standard therapy were included in the study if they had an Eastern Cooperative Oncology Group performance status of <2, a life expectancy of ≥ 3 months, and adequate or acceptable liver (serum bilirubin concentration of $\leq 2\times$ the upper limit of normal, and both aspartate aminotransferase and alanine aminotransferase levels in serum of $\leq 2.5\times$ the upper limit of normal) and bone marrow (absolute white blood cell count of $\geq 3000/mm^3$ and platelet count of $\geq 100\,000/mm^3$) function. Patients were excluded if they had symptomatic brain metastases, active bleeding, malignant ascites requiring drainage, or serious medical conditions such as uncontrolled hypertension, arrhythmia, or heart failure, or if they had been treated with an investigational drug within 4 weeks prior to study enrolment. Individuals were excluded if they had serious illness or concomitant non-oncological disease that was difficult to control by medication. All subjects received information about the nature and purpose of the study, and they provided written informed consent in accordance with institutional guidelines.

Study design. The study was designed as a single-center, open-label, dose-escalation phase I trial. The primary objective was to evaluate the tolerability-safety and dose-limiting toxicity (DLT) of elpamotide. Secondary objectives included determination of the maximum tolerated dose, preliminary assessment of antitumor activity and effects on peripheral blood biomarkers of angiogenesis in this patient population. The study was approved by the appropriate Institutional Review Board. Dose levels of elpamotide were 0.5, 1.0, and

[4]To whom correspondence should be addressed.
E-mail: knishio@med.kindai.ac.jp

doi: 10.1111/cas.12014

2.0 mg per body injected s.c. once a week on a 28-day cycle. Intrapatient dose escalation was not permitted. If a patient experienced a drug-related DLT, the treatment with elpamotide was discontinued. The dose escalation–reduction scheme was based on the occurrence of drug-related DLTs within the first treatment cycle. If a DLT was not observed in any of the first three patients, the dose was escalated to the next level. If a DLT was observed in one of the first three patients, three additional patients were recruited to that dose level. If a DLT occurred in only one of the first six patients, dose escalation was permitted. If two or more of the six patients experienced a DLT, an independent data monitoring committee determined the dose escalation or reduction decision or stopped the recruitment of additional patients.

Safety and efficacy assessments. The safety and tolerability of elpamotide were assessed according to the Common Toxicity Criteria for Adverse Events version 3.0. A DLT was defined as a hematologic toxicity of grade 4 or a non-hematologic toxicity of grade 3 or 4. Objective tumor response was evaluated according to the Response Evaluation Criteria in Solid Tumors version 1.0.[8]

Circulating level of soluble VEGFR2. The concentration of soluble VEGFR2 (sVEGFR2) in serum was measured with ELISA (THERMOmax; Molecular Devices, Sunnyvale, CA, USA) before vaccination on day 1 and after OTS102 administration on days 8 and 29.

Microarray analysis. The PBMCs were isolated from 3 mL whole blood with the use of an Accuspin system (Sigma-Aldrich, St. Louis, MO, USA) and were then immediately suspended in an RNA stabilization solution (Isogen; Nippongene, Tokyo, Japan) and stored at −80°C. Total RNA was subsequently extracted from the cells and its quality checked as described previously.[9] The RNA was subjected to microarray analysis (Affymetrix, Santa Clara, CA, USA) as described.[10] Analysis of the microarray data was carried out with BRB ArrayTools software version 3.6.1 (http://linus.nci.nih.gov/BRB-ArrayTools.html) developed by R. Simon and A. Peng. In brief, a $\log_2$ transformation was applied to the raw data, and global normalization was used to calculate the median expression level over the entire array. Genes were excluded if the proportion of data missing or filtered out was >20%. Genes that passed the filtering criteria were then considered for further analysis. Pathway (gene set) analysis was carried out with the BRB ArrayTools software. The level of statistical significance was set at $P = 0.01$. A P-value was first computed for each gene, and the set of P-values was then summarized by LS and KS statistics. The gene set comparison tool analyzes 285 predefined BioCarta gene sets for differential expression among predefined classes (pre- *vs.* post-treatment).

Other statistical analysis. Serum sVEGFR2 levels at baseline (pretreatment) were compared with those on days 8 or 29 with Student's paired t-test. A P-value of <0.05 was considered statistically significant.

Results

Patient demographics. The characteristics of the 10 HLA-A*24:02-positive patients enrolled in the study are shown in Table 1. The patients included four with non-small-cell lung cancer, three with gastric cancer, two with colorectal cancer, and one with thyroid cancer, all of whom were refractory to standard therapy. Doses of elpamotide for the escalation protocol included 0.5, 1.0, and 2.0 mg. Nine patients completed the first cycle of four injections with elpamotide, with one patient at the dose level of 2.0 mg being withdrawn from the study after two doses of the vaccine because of disease progression. Five patients were subjected to further cycles of vaccination. The median duration of treatment was 58 days (range, 14–279 days), with a median of 8 (range, 2–33) elpamotide vaccinations.

Table 1. Characteristics of HLA-A*24:02-positive patients with advanced refractory solid tumors (n = 10) vaccinated with elpamotide

Characteristics	Peptide dose		
	0.5 mg (n = 3)	1.0 mg (n = 3)	2.0 mg (n = 4)
Median age (range), years	58 (58–65)	64 (58–70)	57 (30–84)
Male/female	1/2	1/2	3/1
Performance status (0/1)	1/2	0/3	0/4
Non-small-cell lung cancer	1	1	2
Gastric cancer	0	1	2
Colorectal cancer	1	1	0
Thyroid cancer	1	0	0

Safety. All 10 patients received at least one dose of the study treatment and were evaluated for safety (Table 2). No patient showed a toxicity of grade 3 or higher. Five patients (50%) (two in the 0.5 mg cohort, one in the 1.0 mg cohort, and two in the 2.0 mg cohort) developed immunologic reactions, erythema, or induration of grade 1 or 2 at injection sites. In the 1.0 mg cohort, one patient developed proteinuria of grade 1 and another developed both hypertension and proteinuria of grade 1. No DLT was thus observed in the trial.

Tumor response. Nine patients were evaluated for tumor response. Although no complete or partial response was observed, two patients had stable disease for at least two treatment cycles (56 days). A 58-year-old female patient with advanced thyroid cancer who had multiple metastases in her lungs and muscle achieved stable disease that persisted for >5 months after the 15th vaccination with elpamotide at 0.5 mg. A 70-year-old male with advanced gastric cancer had been treated with three prior chemotherapy regimens. Given that the tumor continued to grow despite chemotherapy, he was enrolled in the elpamotide 1.0 mg cohort. Tumor size as evaluated by computed tomography remained stable for 2 months after initiation of elpamotide treatment, with stable disease being declared after the eighth vaccination. The patient subsequently received another cycle of four vaccinations. During this third cycle of treatment, ascites was detected by computed tomography and progressive disease was declared.

Pathway analysis. To determine whether elpamotide vaccination induced systemic immunologic effects, we examined the gene expression profiles of PBMCs from all 10 patients before

Table 2. Summary of toxicities of grades (G) 1/2 or 3

Adverse events	Peptide dose						Total
	0.5 mg (n = 3)		1.0 mg (n = 3)		2.0 mg (n = 4)		
	G1/2	G3	G1/2	G3	G1/2	G3	
Reaction at injection site	2	0	1	0	2	0	5
Nasopharyngitis	1	0	0	0	1	0	2
Anorexia	1	0	0	0	1	0	2
Nausea	1	0	0	0	0	0	1
Vomiting	1	0	0	0	0	0	1
Diarrhea	0	0	0	0	1	0	1
Fatigue	0	0	1	0	0	0	1
Fever	0	0	0	0	1	0	1
Hypertension	0	0	1	0	0	0	1
Proteinuria	0	0	2	0	0	0	2

doi: 10.1111/cas.12014

vaccination, and on days 8 and 29 after the onset of vaccination. Pathway analysis of microarray data revealed that 17 pathways were selected from among 285 BioCarta pathways at the nominal significance level of $P = 0.01$ for the LS or KS permutation tests (Table 3). The pathways with the most differentially expressed genes included those related to angiogenesis and T cell function (Table 3), supporting the notion that elpamotide vaccination indeed affects angiogenesis and T cell activation in the clinical setting.

Serum level of sVEGFR2. The circulating level of sVEGFR2 was previously found to be reduced by other angiogenesis inhibitors that directly target VEGFR2. We determined the serum concentration of sVEGFR2 as a potential biomarker for elpamotide vaccination. The serum concentration of sVEGFR2 decreased significantly ($P = 0.026$) over the first 4 weeks of treatment (Fig. 1). The decrease in sVEGFR2 level tended to be larger at the higher dose levels of elpamotide, although this trend was not significant.

Table 3. Pathways with most differentially expressed genes between pre- and post-treatment among 285 BioCarta pathways

Pathway descriptions	No. of genes	LS *P*-value	KS *P*-value	Related pathways
VEGF, hypoxia, and angiogenesis	23	0.0018	0.0270	Angiogenesis
Hypoxia-inducible factor in the cardiovascular system	26	0.0055	0.0023	Angiogenesis
Role of nicotinic acetylcholine	13	0.0075	0.1485	N/A
Melanocyte development and pigmentation pathway	14	0.0093	0.1461	N/A
Transcription regulation by methyltransferase of *CARM1*	20	0.0097	0.0378	N/A
Classical complement pathway	6	0.0141	0.0018	N/A
Role of Tob in T cell activation	26	0.0146	0.0097	T cell
Lectin-induced complement pathway	6	0.0180	0.0018	N/A
Deregulation of CDK5 in Alzheimer's disease	20	0.0193	0.0054	N/A
IL-12- and Stat4-dependent signaling pathway in Th1 development	37	0.0254	0.0078	T cell
T cell receptor and CD3 complex	15	0.0283	0.0023	T cell
NOS2-dependent IL-12 pathway in NK cells	14	0.0350	0.0031	T cell
T cytotoxic cell surface molecules	28	0.0354	0.0072	T cell
T helper cell surface molecules	28	0.0354	0.0072	T cell
Role of MEF2D in T cell apoptosis	31	0.0358	0.0097	T cell
HIV-induced T cell apoptosis	24	0.0442	0.0012	T cell
ADP-ribosylation factor	38	0.0485	0.0087	N/A

CARM1, coactivator-associated arginine methyltransferase 1; IL, interleukin; NK, natural killer; Stat4, signal transducer and activator of transcription-4; N/A, not applicable; VEGF, vascular endothelial growth factor.

Discussion

The targeting of tumor angiogenesis with vaccines has potential advantages over such targeting of tumor cells directly in cancer therapy.[4–6,11] First, tumor endothelial cells are more accessible to the immune system than are tumor cells located at a distance from the vessels.[12] Tumor endothelial cells are thus readily accessed by lymphocytes in the bloodstream, and CTLs can directly damage endothelial cells without penetration into the tumor tissue. In addition, the lysis of even a small number of endothelial cells within the tumor vasculature may result in the disruption of vessel integrity, leading to inhibition of the growth of numerous tumor cells. Endothelial cells are thus a promising target for cancer immunotherapy. Second, the loss or downregulation of HLA molecules on tumor cells is thought to be a major reason for the limited clinical efficacy of vaccines that target tumor cells.[13–15] Given that such HLA loss has not been described for endothelial cells of newly formed tumor vessels, the development of vaccines that target vascular endothelial cells in tumor tissue may overcome the problem of immune-escape of tumor cells.

Vascular endothelial growth factor receptor 2 is a functional molecule associated with neovascularization and is highly expressed in newly-induced tumor vessels but not in normal vessels. The VEGFR2-169 peptide (elpamotide) derived from VEGFR2 has been previously characterized by induction of peptide-specific CTLs capable of killing VEGFR2-expressing human endothelial cells.[6,7] The present phase I study was carried out to examine the safety of elpamotide for HLA-A*24:02-positive patients with advanced tumors. Injection site reactions of grade 1 or 2 were the most frequent vaccine-related adverse events. Specific toxicities that have often been associated with anti-angiogenic treatment with antibodies to VEGF or VEGFR tyrosine kinase inhibitors include hyperten-

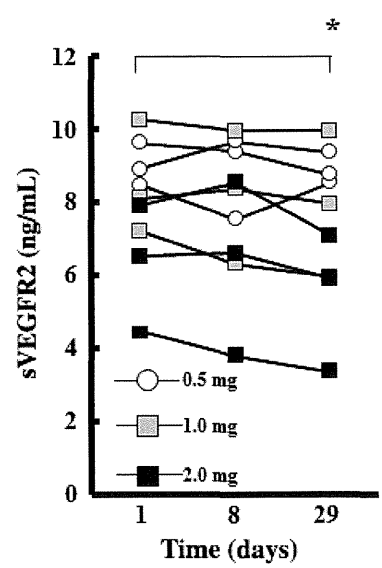

Fig. 1. Serum concentrations of soluble vascular endothelial growth factor receptor 2 (sVEGFR2) before and after elpamotide vaccination. Serum samples were collected at baseline (day 1) as well on days 8 and 29 for determination of sVEGFR2 concentration. *$P = 0.026$ (paired *t*-test) for comparison of the mean values for nine patients between days 1 and 29.

sion and proteinuria.[16,17] These toxicities occurred only at a low grade in two patients in the present study. No adverse events of grade 3 or higher were observed, indicating that elpamotide vaccination is safe and well tolerated.

Although *ex vivo* and *in vitro* studies have provided insight into the specific effects of peptide immunotherapy, they cannot substitute for studies carried out *in vivo*. To date, however, there has been no valid and widely accepted *in vivo* analysis to achieve proof of concept during clinical development of cancer vaccines. Microarray technology has allowed the identification of genes related to a given process in a hypothesis-free approach. The recent introduction of this technology to the field of cancer research has provided insights related to the more accurate classification of cancer, better definition of prognosis, and novel approaches to therapy. Microarray analysis has also proved to be a powerful tool for the identification and characterization of genes related to the ontogeny, differentiation, and activation of immune cells.[18] We have now applied such analysis to PBMCs obtained from patients in order to monitor the biological activity of elpamotide. To facilitate the interpretation of the enormous amount of microarray data, we examined gene sets related to biologically relevant pathways rather than individual genes. The results of our analysis indicate that several pathways related to T cell function and angiogenesis were significantly affected by a single treatment with elpamotide, supporting the notion that this peptide induces an immune response that targets angiogenesis. Our present study thus suggests that microarray analysis is a promising approach to achieving proof of concept during early clinical trials of cancer vaccines. We further explored if the changes in gene expression correlated with treatment response; however, definitive differences between responders (stable disease) ($n = 2$) and non-responders ($n = 7$) were not detected, perhaps due to small sample size. Further investigation to validate whether it will be useful for monitoring the treatment response is warranted.

Given that most angiogenesis inhibitors are cytostatic, it has been difficult to assess the biological effects of these agents in the early phase of clinical trials. Therefore, there is a need for validated biomarkers to monitor biological activity. The circulating level of sVEGFR2 was previously found to be reduced by other angiogenesis inhibitors that directly target VEGFR2,[19–21] although the mechanism underlying this consistent effect is not fully understood.[16,17] In the present study, serum sVEGFR2 concentrations showed a time-dependent decrease at all elpamotide dose levels studied, and this effect tended to be greater at the higher dose levels, suggesting that sVEGFR2 is a potential pharmacodynamic marker of drug exposure.

Inhibition of angiogenesis has provided new treatment avenues for cancer patients; however, there are no reliable biomarkers available to predict therapy response. Although tumor evaluation was not the primary objective of the present study, and the small sample size precludes any conclusions regarding treatment efficacy, the identification of predictive biomarkers to stratify cancer patients is vital to move this anti-angiogenic vaccine therapy forward. A randomized, controlled clinical trial of elpamotide for advanced cancer patients is being carried out in an effort to find such biomarkers.

In conclusion, elpamotide shows an acceptable safety profile for patients with advanced solid tumors. The preliminary evaluation of the biological activity of elpamotide with the use of microarray analysis as well as our serum marker (sVEGFR2) and disease stabilization data indicate that this agent is indeed biologically active.

Acknowledgments

We thank R. Simon and A. Peng for providing the BRB ArrayTools software.

Disclosure Statement

Takuya Tsunoda was employed in a leadership position by OncoTherapy Science (Tokyo, Japan). Kazuhiko Nakagawa received research funding for this study from OncoTherapy Science.

References

1 Kerbel R, Folkman J. Clinical translation of angiogenesis inhibitors. *Nat Rev Cancer* 2002; **2**: 727–39.
2 Carmeliet P, Jain RK. Molecular mechanisms and clinical applications of angiogenesis. *Nature* 2011; **473**: 298–307.
3 Tie J, Desai J. Antiangiogenic therapies targeting the vascular endothelial growth factor signaling system. *Crit Rev Oncog* 2012; **17**: 51–67.
4 Li Y, Wang MN, Li H *et al.* Active immunization against the vascular endothelial growth factor receptor flk1 inhibits tumor angiogenesis and metastasis. *J Exp Med* 2002; **195**: 1575–84.
5 Niethammer AG, Xiang R, Becker JC *et al.* A DNA vaccine against VEGF receptor 2 prevents effective angiogenesis and inhibits tumor growth. *Nat Med* 2002; **8**: 1369–75.
6 Wada S, Tsunoda T, Baba T *et al.* Rationale for antiangiogenic cancer therapy with vaccination using epitope peptides derived from human vascular endothelial growth factor receptor 2. *Cancer Res* 2005; **65**: 4939–46.
7 Miyazawa M, Ohsawa R, Tsunoda T *et al.* Phase I clinical trial using peptide vaccine for human vascular endothelial growth factor receptor 2 in combination with gemcitabine for patients with advanced pancreatic cancer. *Cancer Sci* 2010; **101**: 433–9.
8 Therasse P, Arbuck SG, Eisenhauer EA *et al.* New guidelines to evaluate the response to treatment in solid tumors (RECIST Guidelines). *J Natl Cancer Inst* 2000; **92**: 205–16.
9 Yamanaka R, Arao T, Yajima N *et al.* Identification of expressed genes characterizing long-term survival in malignant glioma patients. *Oncogene* 2006; **25**: 5994–6002.
10 Yamada Y, Arao T, Gotoda T *et al.* Identification of prognostic biomarkers in gastric cancer using endoscopic biopsy samples. *Cancer Sci* 2008; **99**: 2193–9.
11 Ishizaki H, Tsunoda T, Wada S *et al.* Inhibition of tumor growth with antiangiogenic cancer vaccine using epitope peptides derived from human vascular endothelial growth factor receptor 1. *Clin Cancer Res* 2006; **12**: 5841–9.
12 Matejuk A, Leng Q, Chou ST *et al.* Vaccines targeting the neovasculature of tumors. *Vasc Cell* 2011; **3**: 7.
13 Cormier JN, Hijazi YM, Abati A *et al.* Heterogeneous expression of melanoma-associated antigens and HLA-A2 in metastatic melanoma in vivo. *Int J Cancer* 1998; **75**: 517–24.
14 Hicklin DJ, Marincola FM, Ferrone S. HLA class I antigen downregulation in human cancers: T-cell immunotherapy revives an old story. *Mol Med Today* 1999; **5**: 178–86.
15 Paschen A, Mendez RM, Jimenez P *et al.* Complete loss of HLA class I antigen expression on melanoma cells: a result of successive mutational events. *Int J Cancer* 2003; **103**: 759–67.
16 Bertolini F, Shaked Y, Mancuso P *et al.* The multifaceted circulating endothelial cell in cancer: towards marker and target identification. *Nat Rev Cancer* 2006; **6**: 835–45.
17 Brown AP, Citrin DE, Camphausen KA. Clinical biomarkers of angiogenesis inhibition. *Cancer Metastasis Rev* 2008; **27**: 415–34.
18 Monsurro V, Marincola FM. Microarray analysis for a comprehensive immunological-status evaluation during cancer vaccine immune monitoring. *J Biomed Biotechnol* 2011; **2011**: 307297.
19 Drevs J, Siegert P, Medinger M *et al.* Phase I clinical study of AZD2171, an oral vascular endothelial growth factor signaling inhibitor, in patients with advanced solid tumors. *J Clin Oncol* 2007; **25**: 3045–54.
20 Norden-Zfoni A, Desai J, Manola J *et al.* Blood-based biomarkers of SU11248 activity and clinical outcome in patients with metastatic imatinib-resistant gastrointestinal stromal tumor. *Clin Cancer Res* 2007; **13**: 2643–50.
21 Okamoto I, Kaneda H, Satoh T *et al.* Phase I safety, pharmacokinetic, and biomarker study of BIBF 1120, an oral triple tyrosine kinase inhibitor in patients with advanced solid tumors. *Mol Cancer Ther* 2010; **9**: 2825–33.

doi: 10.1111/cas.12014

Published OnlineFirst June 22, 2012; DOI: 10.1158/1535-7163.MCT-11-0934

Molecular Cancer Therapeutics

Antitumor Action of the MET Tyrosine Kinase Inhibitor Crizotinib (PF-02341066) in Gastric Cancer Positive for *MET* Amplification

Wataru Okamoto, Isamu Okamoto, Tokuzo Arao, et al.

Mol Cancer Ther 2012;11:1557-1564. Published OnlineFirst June 22, 2012.

Published OnlineFirst June 22, 2012; DOI: 10.1158/1535-7163.MCT-11-0934

Molecular Cancer Therapeutics

Preclinical Development

Antitumor Action of the MET Tyrosine Kinase Inhibitor Crizotinib (PF-02341066) in Gastric Cancer Positive for *MET* Amplification

Wataru Okamoto[1], Isamu Okamoto[1], Tokuzo Arao[2], Kiyoko Kuwata[1], Erina Hatashita[1], Haruka Yamaguchi[1], Kazuko Sakai[2], Kazuyoshi Yanagihara[3], Kazuto Nishio[2], and Kazuhiko Nakagawa[1]

Abstract

Therapeutic strategies that target the tyrosine kinase MET hold promise for gastric cancer, but the mechanism underlying the antitumor activity of such strategies remains unclear. We examined the antitumor action of the MET tyrosine kinase inhibitor crizotinib (PF-02341066) in gastric cancer cells positive or negative for *MET* amplification. Inhibition of MET signaling by crizotinib or RNA interference–mediated MET depletion resulted in induction of apoptosis accompanied by inhibition of AKT and extracellular signal–regulated kinase phosphorylation in gastric cancer cells with *MET* amplification but not in those without it, suggesting that MET signaling is essential for the survival of *MET* amplification–positive cells. Crizotinib upregulated the expression of BIM, a proapoptotic member of the Bcl-2 family, as well as downregulated that of survivin, X-linked inhibitor of apoptosis protein (XIAP), and c-IAP1, members of the inhibitor of apoptosis protein family, in cells with *MET* amplification. Forced depletion of BIM inhibited crizotinib-induced apoptosis, suggesting that upregulation of BIM contributes to the proapoptotic effect of crizotinib. Crizotinib also exhibited a marked antitumor effect in gastric cancer xenografts positive for *MET* amplification, whereas it had little effect on those negative for this genetic change. Crizotinib thus shows a marked antitumor action both *in vitro* and *in vivo* specifically in gastric cancer cells positive for *MET* amplification. *Mol Cancer Ther; 11(7); 1557–64. ©2012 AACR.*

Introduction

Gastric cancer is the second most frequent cause of cancer deaths worldwide (1). Chemotherapy has a beneficial effect on survival in individuals with advanced-stage gastric cancer, but even so overall survival is usually still only about 1 year (1, 2). Substantial advances in the development of molecularly targeted therapies for gastric cancer have been achieved in recent years (3). Amplification of the proto-oncogene *MET* is a frequent molecular abnormality in gastric cancer (4–6), and a MET-tyrosine kinase inhibitor (TKI) has been shown to induce apoptosis in gastric cancer cells with *MET* amplification (7, 8).

Crizotinib (PF-02341066; Fig. 1A) was recently approved by the U.S. Food and Drug Administration (FDA) for the treatment of patients with lung cancer positive for fusion of the echinoderm microtubule-associated protein–like 4 (*EML4*) and anaplastic lymphoma kinase (*ALK*) genes. This agent also inhibits MET in addition to oncogenic fusion variants of the tyrosine kinase ALK (9, 10), and it may thus be an attractive therapeutic option for individuals with gastric cancer positive for *MET* amplification. We have therefore now investigated the effects of crizotinib on cell survival and signal transduction in gastric cancer cells with *MET* amplification. We further examined the molecular mechanism underlying the antitumor action of MET inhibition.

Authors' Affiliations: Departments of [1]Medical Oncology and [2]Genome Biology, Kinki University Faculty of Medicine, Osaka-Sayama, Osaka; and [3]Laboratory of Health Sciences, Department of Life Sciences, Yasuda Women's University Faculty of Pharmacy, Asaminami, Hiroshima, Japan

Note: Supplementary data for this article are available at Molecular Cancer Therapeutics Online (http://mct.aacrjournals.org/).

Corresponding Author: Isamu Okamoto, Department of Medical Oncology, Kinki University Faculty of Medicine, 377-2 Ohno-higashi, Osaka-Sayama, Osaka 589-8511, Japan. Phone: 81-72-366-0221; Fax: 81-72-360-5000; E-mail: chi-okamoto@dotd.med.kindai.ac.jp

doi: 10.1158/1535-7163.MCT-11-0934

Materials and Methods

Cell culture and reagents

Human gastric cancer cell lines positive (SNU5, Hs746T, MKN45, HSC58, 58As1, 58As9) or negative (SNU1, N87, AGS, MKN1, MKN7, NUGC3, AZ521, MKN28, HSC39, SNU216) for *MET* amplification were obtained as previously described (8, 11). All cells were cultured under a humidified atmosphere of 5% CO_2 at 37°C in RPMI-1640 medium (Sigma) supplemented with 10% FBS and were passaged for ≤3 months before renewal from frozen early-passage stocks obtained from the respective sources. Cells were regularly screened for mycoplasma with the use of a MycoAlert Mycoplasma detection kit (Lonza). Crizotinib was kindly provided by

Published OnlineFirst June 22, 2012; DOI: 10.1158/1535-7163.MCT-11-0934

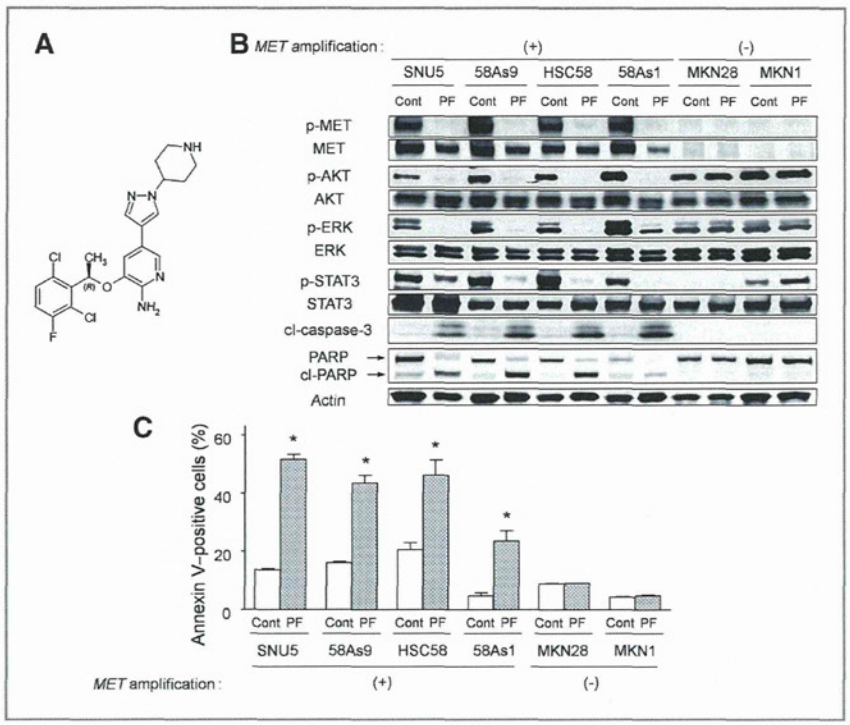

Figure 1. Effects of crizotinib on MET, AKT, ERK, and STAT3 phosphorylation, as well as on apoptosis in human gastric cancer cells. A, structure of crizotinib. B, the indicated cell lines were incubated in the absence (Cont) or presence of crizotinib (PF; 200 nmol/L) for 48 hours, after which cell lysates were prepared and subjected to immunoblot analysis with antibodies to phosphorylated (p) or total forms of MET, AKT, ERK, or STAT3, to caspase-3, to PARP, or to β-actin (loading control). The cleaved (cl) forms of caspase-3 and PARP are indicated. C, cells were incubated as in B, after which the number of apoptotic cells was determined by staining with Annexin V followed by flow cytometry. Data are means ± SD from 3 independent experiments. *, $P < 0.05$ versus the corresponding control value.

Pfizer Global Research & Development, and BEZ235 and AZD6244 were from ShangHai Biochempartner.

Immunoblot analysis

Cells were washed twice with ice-cold PBS and then lysed with 1× Cell Lysis Buffer (Cell Signaling Technology) containing 20 mmol/L Tris-HCl (pH 7.5), 150 mmol/L NaCl, 1 mmol/L EDTA (disodium salt), 1 mmol/L EGTA, 1% Triton X-100, 2.5 mmol/L sodium pyrophosphate, 1 mmol/L β-glycerophosphate, 1 mmol/L Na_3VO_4, leupeptin (1 μg/mL), and 1 mmol/L phenylmethylsulfonyl fluoride. The protein concentration of cell lysates was determined with a BCA Protein Assay Kit (Thermo Fisher Scientific), and equal amounts of protein were subjected to SDS-PAGE on a 7.5% or 12% gel (Bio-Rad). The separated proteins were transferred to a nitrocellulose membrane, which was then incubated with Blocking One solution (Nacalai Tesque) for 20 minutes at room temperature before incubation overnight at 4°C with primary antibodies. Rabbit polyclonal antibodies to phosphorylated human MET (pY1234/pY1235), total AKT, phosphorylated AKT, phosphorylated extracellular signal–regulated kinase (ERK), total STAT3, phosphorylated STAT3 (phospho-Tyr705), PARP, caspase-3, BIM, Bcl-2, and X-linked inhibitor of apoptosis protein (XIAP) were obtained from Cell Signaling Technology; those to total ERK were from Santa Cruz Biotechnology; those to total MET were from Zymed/Invitrogen; those to survivin were from Novus; those to c-IAP1 were from R&D Systems; and those to β-actin were from Sigma. All antibodies were used at a 1:1,000 dilution, with the exception of those to β-actin (1:200). The membrane was then washed with PBS containing 0.05% Tween-20 before incubation for 1 hour at room temperature with horseradish peroxidase–conjugated secondary antibodies (GE Healthcare). Immune complexes were finally detected with ECL Western Blotting Detection Reagents (GE Healthcare).

Gene silencing

Cells were plated at 50% to 60% confluence in 6-well plates or 25-cm^2 flasks and then incubated for 24 hours before transient transfection for the indicated times with siRNAs mixed with the Lipofectamine reagent (Invitrogen). The siRNAs specific for MET (MET-1, 5′-ACAAGAUCGUCAACAAAAA-3′; MET-2, 5′-CUACAGAAAUGGUUUCAAA-3′), BIM (BIM-1, 5′-GGAGGGUAUUUUUGAAUAA-3′; BIM-2, 5′-AGGAGGGUAUUUUUGAAUA-3′), or AKT (AKT-1, 5′-CCAGGUAUUUUGAUGAGGA-3′; AKT-2, 5′-CAACCGCCAUCCAGACUGU-3′) mRNAs, as well as corresponding scrambled (control) siRNAs were obtained from Nippon EGT. The data presented for the effects of MET, BIM, or AKT depletion were obtained with the corresponding siRNA-1, but similar results were obtained with each siRNA-2.

Annexin V–binding assay

The binding of Annexin V to cells was measured with the use of an Annexin-V-FLUOS Staining Kit (Roche).

Published OnlineFirst June 22, 2012; DOI: 10.1158/1535-7163.MCT-11-0934

Cells were harvested by exposure to trypsin-EDTA, washed with PBS, and centrifuged at 200 × *g* for 5 minutes. The cell pellets were resuspended in 100 μL of Annexin-V-FLUOS labeling solution, incubated for 10 to 15 minutes at 15° to 25°C, and then analyzed for fluorescence with a flow cytometer (FACSCalibur) and Cell Quest software (Becton Dickinson).

Cell growth inhibition assay

Cells were transferred to 96-well flat-bottomed plates and cultured for 24 hours before exposure to various concentrations of crizotinib for 72 hours. Tetra Color One (5 mmol/L tetrazolium monosodium salt and 0.2 mmol/L 1-methoxy-5-methyl phenazinium methylsulfate; Seikagaku Kogyo) was then added to each well, and the cells were incubated for 3 hours at 37°C before measurement of absorbance at 490 nm with a Multiskan Spectrum instrument (Thermo Labsystems). Absorbance values were expressed as a percentage of that for untreated cells, and the concentration of crizotinib resulting in 50% growth inhibition (IC_{50}) was calculated.

Growth inhibition assay *in vivo*

All animal studies were conducted in accordance with the Recommendations for Handling of Laboratory Animals for Biomedical Research compiled by the Committee on Safety and Ethical Handling Regulations for Laboratory Animal Experiments, Kinki University (Osaka, Japan). The ethical procedures followed conformed to the guidelines of the United Kingdom Co-ordinating Committee on Cancer Research (12). Tumors cells (5×10^6) were injected subcutaneously into the axilla of 5- to 6-week-old female athymic nude mice (BALB/c *nu/nu*; CLEA Japan). Treatment was initiated when tumors in each group of 6 mice achieved an average volume of 300 to 900 mm^3. Treatment groups consisted of vehicle control and crizotinib (25 or 50 mg/kg). Crizotinib was administered by oral gavage daily for 4 weeks, with control animals receiving a 0.5% (w/v) aqueous solution of hydroxypropylmethylcellulose as vehicle. Tumor volume was determined from caliper measurements of tumor length (*L*) and width (*W*) according to the formula $LW^2/2$. Both tumor size and body weight were measured twice per week.

Statistical analysis

Quantitative data are presented as means ± SD or SEM from 3 independent experiments or for 6 animals per group, unless indicated otherwise, and were analyzed with the Student 2-tailed *t* test. A *P* value of <0.05 was considered statistically significant.

Results

Crizotinib inhibits the proliferation of gastric cancer cells with *MET* amplification

We first examined the effect of the MET-TKI crizotinib on the proliferation of gastric cancer cells positive or negative for *MET* amplification. Six cell lines with *MET* amplification (MKN45, HSC58, 58As1, 58As9, SNU5, Hs746T) were sensitive to crizotinib, with IC_{50} values of less than 200 nmol/L (Table 1). In contrast, crizotinib did not substantially inhibit the proliferation of gastric cancer cells without such gene amplification (Table 1). Transcripts of the *EML4–ALK* fusion gene were not detected in the crizotinib-sensitive gastric cancer cell lines by reverse transcription PCR analysis (data not shown). These data suggested that crizotinib has a marked antiproliferative effect specifically in gastric cancer cells with *MET* amplification.

Table 1. IC_{50} values of crizotinib for inhibition of the growth of gastric cancer cells *in vitro*

Crizotinib response	Cell line	Crizotinib IC_{50}, μmol/L	*MET* amplification
Sensitive	MKN45	0.04	+
	HSC58	0.05	+
	58As1	0.06	+
	58As9	0.17	+
	SNU5	0.03	+
	Hs746T	0.05	+
Resistant	MKN1	8.57	–
	AZ521	1.96	–
	SNU216	4.19	–
	N87	6.10	–
	MKN7	>10	–
	SNU1	0.80	–
	HSC39	2.75	–
	AGS	0.90	–
	MKN28	3.73	–
	NUGC3	2.65	–

NOTE: Data are means of triplicates from experiments that were repeated a total of 3 times with similar results.

Effects of crizotinib on downstream signaling of MET and on apoptosis in gastric cancer cells with or without *MET* amplification

We next examined the effects of crizotinib on phosphorylation of ERK, AKT, and STAT3 in gastric cancer cell lines. Crizotinib markedly inhibited the phosphorylation of ERK, AKT, and STAT3, as well as that of MET in cells with *MET* amplification (Fig. 1B; Supplementary Fig. S1). In contrast, crizotinib had little effect on the phosphorylation of ERK, AKT, or STAT3 in gastric cancer cells without amplification of *MET* (Fig. 1B). Determination of cell-cycle distribution in SNU5, HSC58, 58As1, and 58As9 cells, all of which manifest *MET* amplification, revealed that treatment with crizotinib for 72 hours increased the size of the cell population in sub-G_1 phase, indicative of the induction of apoptosis, as well as reduced that of the cell population in S-phase (Supplementary Fig. S2). We further investigated the effect of crizotinib on apoptosis.

Published OnlineFirst June 22, 2012; DOI: 10.1158/1535-7163.MCT-11-0934

Immunoblot analysis showed that crizotinib triggered the generation of the cleaved forms of caspase-3 and PARP in cells with *MET* amplification but not in those without it (Fig. 1B). Consistent with these results, an Annexin V–binding assay revealed that crizotinib induced a substantial level of apoptosis in *MET* amplification–positive cells but was largely without effect in cell lines without *MET* amplification (Fig. 1C). These data thus suggested that crizotinib inhibits the phosphorylation of ERK, AKT, and STAT3, resulting in induction of apoptosis, in gastric cancer cells with *MET* amplification, whereas such effects were not observed in cells without *MET* amplification.

Effects of crizotinib on the expression of apoptosis-related proteins in *MET* amplification–positive gastric cancer cells

Given that crizotinib induced apoptosis in *MET* amplification–positive gastric cancer cells, we examined the effects of this drug on the expression of apoptosis-related proteins in such cells. Crizotinib upregulated the expression of BIM, a proapoptotic member of the Bcl-2 family of proteins, whereas it had little effect on the expression of other Bcl-2 family members including Bcl-2 (Fig. 2A). Furthermore, crizotinib downregulated the expression of members of the IAP family including survivin, XIAP, and c-IAP1 in cells with *MET* amplification (Fig. 2A).

To verify that the effects of crizotinib on the expression of apoptosis-related proteins in *MET* amplification–positive gastric cancer cells are indeed mediated by MET inhibition rather than by nonspecific inhibition of other kinases, we transfected gastric cancer cells with siRNAs specific for MET mRNA. Transfection with MET siRNAs resulted in a marked decrease in the abundance of MET, which was accompanied by generation of the cleaved forms of both caspase-3 and PARP, in SNU5 and 58As9 cells, both of which manifest *MET* amplification (Fig. 2B). Similar to the effects of crizotinib, depletion of MET by RNA interference (RNAi) also resulted in upregulation of BIM and downregulation of members of the IAP family, whereas it had little effect on the expression of Bcl-2 in such cells (Fig. 2B). These data thus suggested that the upregulation of BIM and the downregulation of members of the IAP family, including survivin, XIAP, and c-IAP1, are related to the induction of apoptosis by the MET inhibitor in gastric cancer cells with *MET* amplification.

Inhibition of the MEK-ERK or PI3K-AKT pathways results in BIM upregulation and survivin downregulation, respectively, in *MET* amplification–positive cells

To identify the signaling pathways responsible for upregulation or downregulation of apoptosis-related proteins by crizotinib, we examined the effects of specific inhibitors of the mitogen-activated protein (MAP)/ERK kinase (MEK) and of phosphoinositide 3-kinase (PI3K) in *MET* amplification–positive cell lines. The MEK inhibitor AZD6244 induced BIM expression without affecting the abundance of the other proteins examined (Fig. 3A), suggesting that expression of BIM is regulated by the MEK-ERK pathway. On the other hand, the PI3K inhibitor BEZ235 reduced the abundance of survivin without affecting that of the other IAP family proteins including c-IAP1 and XIAP (Fig. 3A). We also found that depletion of AKT by RNAi resulted in downregulation of survivin but not of XIAP or c-IAP1 in the *MET* amplification–positive SNU5 and 58As9 cell lines (Fig. 3B). Together, these data suggested that crizotinib regulates BIM and survivin expression through inhibition of the MEK-ERK and PI3K-AKT signaling pathways, respectively, in *MET* amplification–positive gastric cancer cells.

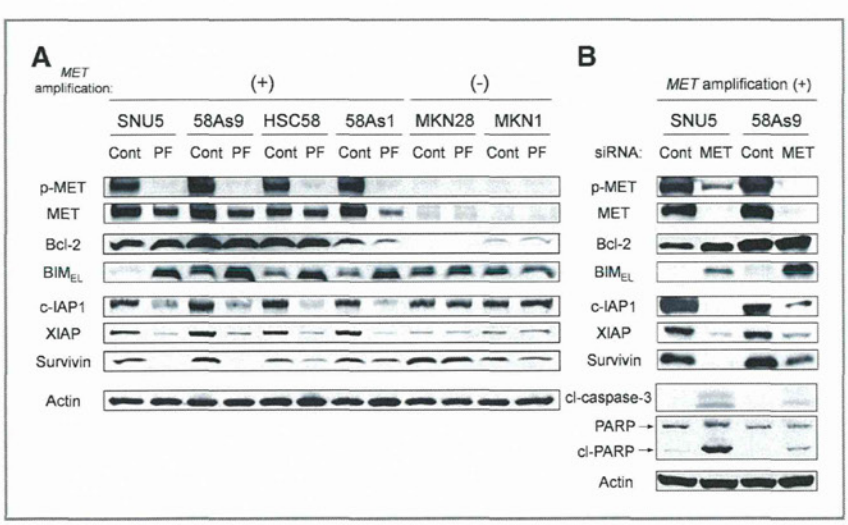

Figure 2. Effects of MET inhibition or depletion on the expression of Bcl-2 family and IAP family proteins in human gastric cancer cells. The indicated cell lines were incubated with or without crizotinib (200 nmol/L) for 24 hours (A) or were transfected with nonspecific (Cont) or MET siRNAs for 48 hours (B), after which cell lysates were prepared and subjected to immunoblot analysis with antibodies to the indicated proteins. The position of the band corresponding to BIM_{EL} is indicated.

Published OnlineFirst June 22, 2012; DOI: 10.1158/1535-7163.MCT-11-0934

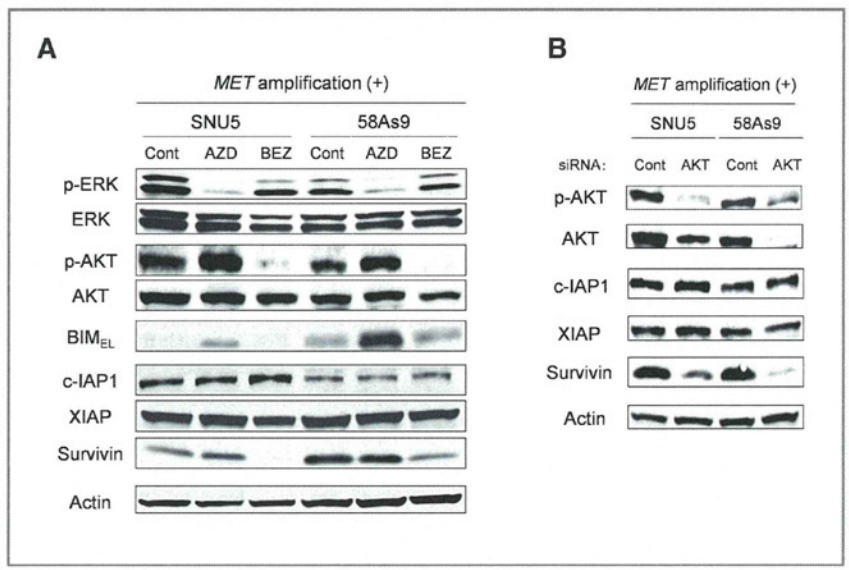

Figure 3. Effects of inhibition of the MEK-ERK or PI3K-AKT signaling pathways on the expression of Bcl-2 family and IAP family proteins in *MET* amplification–positive gastric cancer cells. The indicated cell lines were incubated in the absence (Cont, 0.1% dimethyl sulfoxide) or presence of AZD6244 (0.2 μmol/L) or BEZ235 (0.2 μmol/L) for 24 hours (A) or were transfected with nonspecific (Cont) or AKT siRNAs for 48 hours (B), after which cell lysates were prepared and subjected to immunoblot analysis with antibodies to the indicated proteins.

Role of BIM induction in crizotinib-induced apoptosis in gastric cancer cells with *MET* amplification

Induction of the proapoptotic BH3-only protein BIM has been found to be important for TKI-induced apoptosis in EGF receptor (*EGFR*) gene mutation–positive lung cancer and *HER2* amplification–positive breast cancer (13–17). To investigate whether the upregulation of BIM is related to the induction of apoptosis by crizotinib, we transfected *MET* amplification–positive gastric cancer cells with siRNAs specific for BIM mRNAs. Such transfection resulted in marked inhibition of the upregulation of BIM by crizotinib (Fig. 4A). Immunoblot analysis showed that the attenuation of BIM induction was associated with inhibition of crizotinib-induced apoptosis, as revealed by a reduced extent of caspase-3 and PARP cleavage (Fig. 4A). The Annexin V–binding assay also revealed that such transfection resulted in inhibition of crizotinib-induced apoptosis (Fig. 4B). These data thus suggested that the induction of apoptosis by crizotinib in gastric cancer cells with *MET* amplification is mediated, at least in part, by upregulation of BIM.

Effect of crizotinib on the growth of gastric cancer cells *in vivo*

To determine whether the antitumor action of crizotinib observed *in vitro* might also be apparent *in vivo*, we injected 58As9 cells (positive for *MET* amplification),

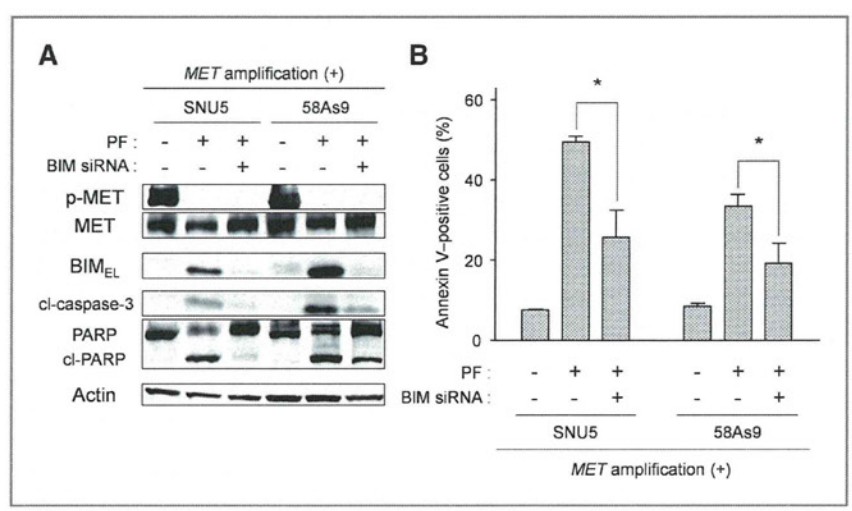

Figure 4. Effect of BIM depletion on apoptosis induced by crizotinib in gastric cancer cells with *MET* amplification. A, the indicated cell lines were transfected with BIM or nonspecific siRNAs for 24 hours and then incubated for 48 hours with or without crizotinib (200 nmol/L). The cells were then lysed and subjected to immunoblot analysis with antibodies to the indicated proteins. B, cells treated as in (A) were assayed for apoptosis by staining with Annexin V followed by flow cytometry. Data are means ± SD from 3 independent experiments. *, $P < 0.05$ for the indicated comparisons.

Published OnlineFirst June 22, 2012; DOI: 10.1158/1535-7163.MCT-11-0934

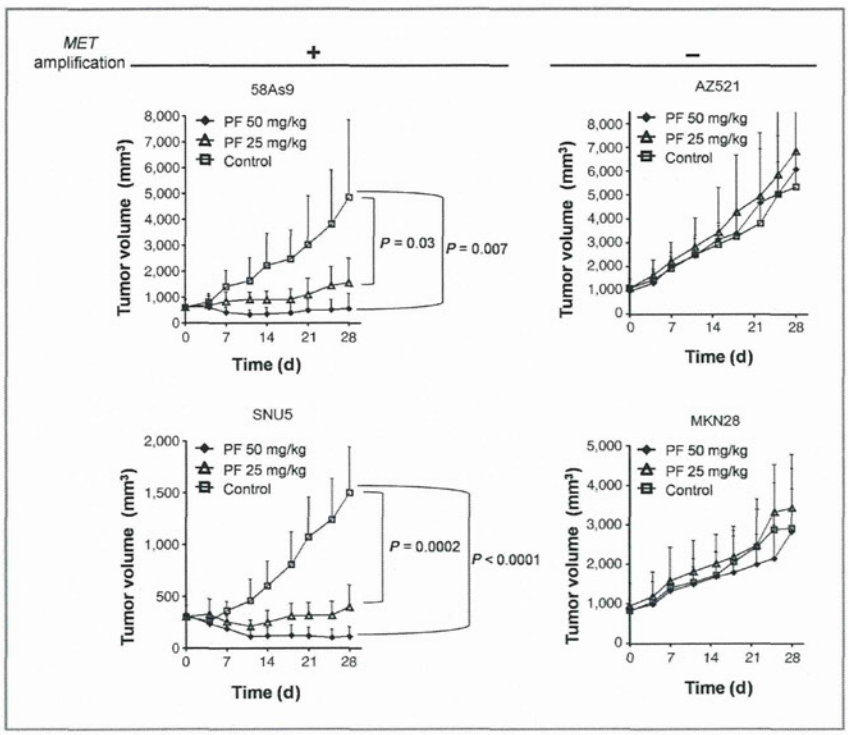

Figure 5. Effect of crizotinib on the growth of gastric cancer cells *in vivo*. Nude mice with tumor xenografts established by subcutaneous injection of 58As9, SNU5, AZ521, or MKN28 cells were treated daily for 4 weeks with vehicle (control) or crizotinib (25 or 50 mg/kg). Tumor volume was determined at the indicated times after the onset of treatment. Data are means ± SEM for 6 mice per group. *P* values are for the indicated comparisons at 28 days.

SNU5 cells (positive for *MET* amplification), AZ521 cells (negative for *MET* amplification), or MKN28 cells (negative for *MET* amplification) into nude mice to elicit the formation of solid tumors. After tumor formation, the mice were treated with vehicle (control) or with crizotinib at a daily dose of 25 or 50 mg/kg by oral gavage for 4 weeks. Crizotinib at either dose eradicated tumors in mice injected with 58As9 or SNU5 cells (Fig. 5; Supplementary Fig. S3). In contrast, tumors in mice injected with AZ521 or MKN28 cells were not affected by crizotinib treatment even at the dose of 50 mg/kg/d (Fig. 5; Supplementary Fig. S3). Treatment with crizotinib at either dose was well-tolerated by the mice, with no signs of toxicity or weight loss during therapy (data not shown). Crizotinib thus exhibited a marked antitumor effect in gastric cancer xenografts positive for *MET* amplification, whereas it had little effect on those negative for *MET* amplification, consistent with our results obtained *in vitro*.

Discussion

Aberrant activation of receptor tyrosine kinase signaling pathways contributes to the development of various types of cancer. Small-molecule inhibitors that target these activated kinases have been developed and have shown substantial efficacy in clinical trials. The identification of patient subgroups that might actually benefit from treatment with such drugs would be expected to optimize their efficacy. The receptor tyrosine kinase MET is considered one such potential target in cancer, and several MET-TKIs are currently undergoing clinical trials in humans. Amplification of *MET* is often responsible for activation of MET signaling, with such amplification occurring frequently in gastric cancer (4–6). We have now shown that crizotinib exerted a marked antitumor action in gastric cancer cells with *MET* amplification. In such gastric cancer cells, attenuation of MET function either by treatment with crizotinib or by MET-targeted RNAi resulted in inhibition of AKT and ERK signaling as well as in the induction of apoptosis, indicating that tumor cells with *MET* amplification are dependent on MET signaling for their growth and survival. Targeting of MET signaling by MET-TKIs is thus a potentially valuable therapeutic strategy for patients with gastric cancer with *MET* amplification.

We also investigated the mediators of crizotinib-induced apoptosis in *MET* amplification–positive gastric cancer cells. We found that crizotinib induced upregulation of BIM, a key proapoptotic member of the Bcl-2 family of proteins that initiates apoptosis signaling by binding to and antagonizing the function of prosurvival Bcl-2 family members (18). Furthermore, depletion of BIM by RNAi resulted in inhibition of crizotinib-induced apoptosis in gastric cancer cells with *MET* amplification, indicating that upregulation of BIM contributes to the induction of apoptosis by the MET-TKI in such cells. These findings are consistent with those of previous studies of lung cancer

Published OnlineFirst June 22, 2012; DOI: 10.1158/1535-7163.MCT-11-0934

cells with *EGFR* mutations and breast cancer cells with *HER2* amplification (13–17). However, our observations revealed that depletion of BIM did not completely abolish crizotinib-induced apoptosis, suggesting that another apoptotic regulator might contribute to MET-TKI–induced apoptotic cell death. We also found that crizotinib induced downregulation of survivin, a member of the IAP family that protects cells against apoptosis by either directly or indirectly inhibiting the activation of effector caspases (19). We found that a PI3K inhibitor or RNAi-mediated depletion of AKT reduced the abundance of survivin, indicating that the expression of survivin is regulated by PI3K-AKT signaling in *MET* amplification–positive gastric cancer cells. Previous studies have shown that the expression of survivin is dependent on PI3K-AKT signaling that operates downstream of receptor tyrosine kinases and is essential for cell survival in *EGFR* mutation–positive non–small cell lung cancer cells as well as in breast cancer cells positive for *HER2* amplification (16, 17). These results suggest that downregulation of survivin via inhibition of the MET-PI3K-AKT pathway likely also contributes to the induction of apoptosis by crizotinib in *MET* amplification–positive gastric cancer cells.

We have shown that crizotinib induced downregulation of XIAP and c-IAP1 in gastric cancer cells with *MET* amplification. We further showed that depletion of MET by RNAi induced downregulation of XIAP and c-IAP1, indicating that these proteins are also regulated by MET signaling in *MET* amplification–positive gastric cancer cells. We investigated which signaling pathway is responsible for downregulation of XIAP and c-IAP1 resulting from inhibition of MET. Given that crizotinib inhibited both ERK and AKT phosphorylation in *MET* amplification–positive cell lines, we examined the effects both of specific inhibitors of MEK and PI3K as well as of siRNAs specific for AKT mRNA in such cells. However, none of these agents induced downregulation of XIAP or c-IAP1 in gastric cancer cells with *MET* amplification. We previously showed that activation of STAT3 is linked to MET signaling and that forced expression of a constitutively active form of STAT3 attenuated MET-TKI–induced apoptosis in MET-activated gastric cancer cells, suggesting that inhibition of STAT3 activity contributes to MET-TKI–induced apoptosis (20). To investigate whether the regulation of XIAP or c-IAP1 expression is mediated by STAT3 signaling, we transfected SNU5 and 58As9 cells, both of which manifest *MET* amplification, with an siRNA that targets STAT3 mRNA. However, depletion of STAT3 by RNAi had no substantial effect on expression of XIAP and c-IAP1 in such cells (data not shown). Previous studies have shown that XIAP and c-IAP1 were not substantially affected by EGFR-TKIs in *EGFR* mutation–positive non–small cell lung cancer cells or by HER2-targeting agents in breast cancer cells positive for *HER2* amplification (16, 17). Given that inhibition of MET results in downregulation of XIAP and c-IAP1 in *MET* amplification–positive gastric cancer cells, the mechanism by which the expression of such proteins is regulated likely differs between MET and other receptor tyrosine kinases including EGFR and HER2. However, the signaling pathway responsible for downregulation of XIAP and c-IAP1 by MET inhibition remains unknown. Further studies are thus required to clarify the regulation of XIAP and c-IAP1 and the contribution of members of the IAP family to MET-TKI–induced apoptosis in gastric cancer cells with *MET* amplification.

In conclusion, our results have shown that crizotinib has pronounced effects on signal transduction and survival in gastric cancer cells with *MET* amplification. Crizotinib has recently been approved for treatment of ALK-driven lung cancer by the FDA on the basis of safety and effectiveness data. The IC_{50} values of crizotinib for inhibition of the growth of *MET* amplification–positive gastric cancer cell lines were lower than the mean trough concentration of the drug achieved in the plasma of patients at steady state (292 ng/mL or 644 nmol/L; ref. 21). Indeed, crizotinib was recently found to exhibit antitumor activity in 2 of 4 patients with *MET* amplification–positive gastroesophageal cancer (22), supporting further study of the molecular mechanism underlying its antitumor action. In the present study, we showed that BIM and IAP family members including survivin, XIAP, and c-IAP1 play a role in crizotinib-induced apoptosis in association with inhibition of MET signaling in gastric cancer cells with *MET* amplification. Our observations provide a basis for the further development of MET-targeted therapy for patients with gastric cancer with *MET* amplification.

Disclosure of Potential Conflicts of Interest

No potential conflicts of interest were disclosed.

Authors' Contributions

Conception and design: W. Okamoto, I. Okamoto, K. Nakagawa
Development of methodology: W. Okamoto, T. Arao, K. Sakai, K. Yanagihara
Acquisition of data (provided animals, acquired and managed patients, provided facilities, etc.): W. Okamoto, I. Okamoto, K. Kuwata, E. Hatashita, H. Yamaguchi, K. Sakai
Analysis and interpretation of data (e.g., statistical analysis, biostatistics, computational analysis): W. Okamoto, I. Okamoto, K. Kuwata, E. Hatashita, H. Yamaguchi
Writing, review, and/or revision of the manuscript: W. Okamoto, I. Okamoto, K. Nishio, K. Nakagawa
Administrative, technical, or material support (i.e., reporting or organizing data, constructing databases): T. Arao, K. Kuwata, E. Hatashita, H. Yamaguchi, K. Sakai, K. Yanagihara
Study supervision: I. Okamoto, K. Nakagawa

Acknowledgments

The authors thank Pfizer for the provision of crizotinib (PF-02341066) used in this study.

Grant Support

The authors received no grant support for this study.

The costs of publication of this article were defrayed in part by the payment of page charges. This article must therefore be hereby marked *advertisement* in accordance with 18 U.S.C. Section 1734 solely to indicate this fact.

Received November 16, 2011; revised March 30, 2012; accepted April 11, 2012; published OnlineFirst June 22, 2012.

Published OnlineFirst June 22, 2012; DOI: 10.1158/1535-7163.MCT-11-0934

References

1. Hartgrink HH, Jansen EP, van Grieken NC, van de Velde CJ. Gastric cancer. Lancet 2009;374:477–90.
2. Wesolowski R, Lee C, Kim R. Is there a role for second-line chemotherapy in advanced gastric cancer? Lancet Oncol 2009;10: 903–12.
3. Bang YJ, Van Cutsem E, Feyereislova A, Chung HC, Shen L, Sawaki A, et al. Trastuzumab in combination with chemotherapy versus chemotherapy alone for treatment of HER2-positive advanced gastric or gastro-oesophageal junction cancer (ToGA): a phase 3, open-label, randomised controlled trial. Lancet 2010;376:687–97.
4. Kuniyasu H, Yasui W, Kitadai Y, Yokozaki H, Ito H, Tahara E. Frequent amplification of the c-met gene in scirrhous type stomach cancer. Biochem Biophys Res Commun 1992;189:227–32.
5. Nessling M, Solinas-Toldo S, Wilgenbus KK, Borchard F, Lichter P. Mapping of chromosomal imbalances in gastric adenocarcinoma revealed amplified protooncogenes MYCN, MET, WNT2, and ERBB2. Genes Chromosomes Cancer 1998;23:307–16.
6. Sakakura C, Mori T, Sakabe T, Ariyama Y, Shinomiya T, Date K, et al. Gains, losses, and amplifications of genomic materials in primary gastric cancers analyzed by comparative genomic hybridization. Genes Chromosomes Cancer 1999;24:299–305.
7. Smolen GA, Sordella R, Muir B, Mohapatra G, Barmettler A, Archibald H, et al. Amplification of MET may identify a subset of cancers with extreme sensitivity to the selective tyrosine kinase inhibitor PHA-665752. Proc Natl Acad Sci U S A 2006;103:2316–21.
8. Okamoto W, Okamoto I, Yoshida T, Okamoto K, Takezawa K, Hatashita E, et al. Identification of c-Src as a potential therapeutic target for gastric cancer and of MET activation as a cause of resistance to c-Src inhibition. Mol Cancer Ther 2010;9:1188–97.
9. Zou HY, Li Q, Lee JH, Arango ME, McDonnell SR, Yamazaki S, et al. An orally available small-molecule inhibitor of c-Met, PF-2341066, exhibits cytoreductive antitumor efficacy through antiproliferative and antiangiogenic mechanisms. Cancer Res 2007;67:4408–17.
10. Tanizaki J, Okamoto I, Okamoto K, Takezawa K, Kuwata K, Yamaguchi H, et al. MET tyrosine kinase inhibitor crizotinib (PF-02341066) shows differential antitumor effects in non-small cell lung cancer according to MET alterations. J Thorac Oncol 2011;6:1624–31.
11. Yanagihara K, Takigahira M, Tanaka H, Komatsu T, Fukumoto H, Koizumi F, et al. Development and biological analysis of peritoneal metastasis mouse models for human scirrhous stomach cancer. Cancer Sci 2005;96:323–32.
12. United Kingdom Co-ordinating Committee on Cancer Research (UKCCCR). Guidelines for the welfare of animals in experimental neoplasia (second edition). Br J Cancer 1998;77:1–10.
13. Costa DB, Halmos B, Kumar A, Schumer ST, Huberman MS, Boggon TJ, et al. BIM mediates EGFR tyrosine kinase inhibitor-induced apoptosis in lung cancers with oncogenic EGFR mutations. PLoS Med 2007;4:1669–79; discussion 1680.
14. Cragg MS, Kuroda J, Puthalakath H, Huang DC, Strasser A. Gefitinib-induced killing of NSCLC cell lines expressing mutant EGFR requires BIM and can be enhanced by BH3 mimetics. PLoS Med 2007;4:1681–89; discussion 1690.
15. Gong Y, Somwar R, Politi K, Balak M, Chmielecki J, Jiang X, et al. Induction of BIM is essential for apoptosis triggered by EGFR kinase inhibitors in mutant EGFR-dependent lung adenocarcinomas. PLoS Med 2007;4:e294.
16. Okamoto K, Okamoto I, Okamoto W, Tanaka K, Takezawa K, Kuwata K, et al. Role of survivin in EGFR inhibitor-induced apoptosis in non-small cell lung cancers positive for EGFR mutations. Cancer Res 2010;70:10402–10.
17. Tanizaki J, Okamoto I, Fumita S, Okamoto W, Nishio K, Nakagawa K. Roles of BIM induction and survivin downregulation in lapatinib-induced apoptosis in breast cancer cells with HER2 amplification. Oncogene 2011;30:4097–106.
18. Chen L, Willis SN, Wei A, Smith BJ, Fletcher JI, Hinds MG, et al. Differential targeting of prosurvival Bcl-2 proteins by their BH3-only ligands allows complementary apoptotic function. Mol Cell 2005;17: 393–403.
19. Hengartner MO. The biochemistry of apoptosis. Nature 2000;407: 770–6.
20. Okamoto W, Okamoto I, Arao T, Yanagihara K, Nishio K, Nakagawa K. Differential roles of STAT3 depending on the mechanism of STAT3 activation in gastric cancer cells. Br J Cancer 2011;105: 407–12.
21. Bang YJ, Kwak EL, Shaw AT, Camidge DR, Iafrate AJ, Maki RG, et al. Clinical activity of the oral ALK inhibitor PF-02341066 in ALK-positive patients with non-small cell lung cancer (NSCLC). J Clin Oncol 28:18s, 2010 (suppl; abstr 3).
22. Lennerz JK, Kwak EL, Ackerman A, Michael M, Fox SB, Bergethon K, et al. MET amplification identifies a small and aggressive subgroup of esophagogastric adenocarcinoma with evidence of responsiveness to crizotinib. J Clin Oncol 2011;29:4803–10.

Annals of Oncology 23: 2914–2919, 2012
doi:10.1093/annonc/mds121
Published online 9 July 2012

An evaluation study of *EGFR* mutation tests utilized for non-small-cell lung cancer in the diagnostic setting

K. Goto[1*], M. Satouchi[2], G. Ishii[3], K. Nishio[4], K. Hagiwara[5], T. Mitsudomi[6], J. Whiteley[7], E. Donald[7], R. McCormack[7] & T. Todo[8]

[1]*Division of Thoracic Oncology, National Cancer Center Hospital East, Chiba;* [2]*Department of Thoracic Oncology, Hyogo Cancer Center, Hyogo;* [3]*Pathology Division, Innovative Medical Research Center, National Cancer Center Hospital East, Chiba;* [4]*Department of Genome Biology, Kinki University School of Medicine, Osaka;* [5]*Department of Respiratory Medicine, Saitama Medical University, Saitama;* [6]*Department of Thoracic Surgery, Aichi Cancer Center Hospital, Aichi, Japan;* [7]*Department of Personalised Healthcare and Biomarkers, AstraZeneca Pharmaceuticals, Macclesfield, UK;* [8]*Department of Research and Development, AstraZeneca KK, Osaka, Japan*

Received 19 December 2011; revised 2 March 2012; accepted 12 March 2012

Background: Epidermal growth factor receptor (*EGFR*) mutation is predictive for the efficacy of EGFR tyrosine kinase inhibitors in advanced non-small-cell lung cancer (NSCLC) treatment. We evaluated the performance, sensitivity, and concordance between five *EGFR* tests.

Materials and methods: DNA admixtures ($n = 34$; 1%–50% mutant plasmid DNA) and samples from NSCLC patients [116 formalin-fixed paraffin-embedded (FFPE) tissue, 29 matched bronchofiberscopic brushing (BB) cytology, and 20 additional pleural effusion (PE) cytology samples] were analyzed. *EGFR* mutation tests were PCR-Invader®, peptide nucleic acid-locked nucleic acid PCR clamp, direct sequencing, Cycleave™, and Scorpion Amplification Refractory Mutation System (ARMS)®. Analysis success, mutation status, and concordance rates were assessed.

Results: All tests except direct sequencing detected four mutation types at ≥1% mutant DNA. Analysis success rates were 91.4%–100% (FFPE) and 100% (BB and PE cytology), respectively. Inter-assay concordance rates of successfully analyzed samples were 94.3%–100% (FFPE; kappa coefficients: 0.88–1.00), 93.1%–100% (BB cytology; 0.86–1.00), and 85.0%–100% (PE cytology; 0.70–1.00), and 93.1%–96.6% (0.86–0.93) between BB cytology and matched FFPE.

Conclusions: All *EGFR* assays carried out comparably in the analysis of FFPE and cytology samples. Cytology-derived DNA is a viable alternative to FFPE samples for analyzing *EGFR* mutations.

Key words: cytology, EGFR mutation, FFPE, NSCLC, PCR

introduction

Epidermal growth factor receptor (*EGFR*) mutation is a key predictive factor for the efficacy of EGFR tyrosine kinase inhibitors in the treatment of patients with advanced non-small-cell lung cancer (NSCLC) [1–3]. *EGFR* mutation testing is necessary to enable the physician to offer the most suitable therapy for a patient with advanced NSCLC.

Four *EGFR* mutation tests, PCR-Invader® [4], peptide nucleic acid-locked nucleic acid (PNA-LNA) PCR clamp [5], PCR direct sequencing [6], and Cycleave PCR™ [7] are used commercially in Japan, with testing generally carried out by centralized contracted laboratories. The Scorpion Amplification Refractory Mutation System (ARMS)® [8] is another sensitive globally available method and in particular was used in the phase III Iressa Pan-Asia Study (IPASS) to determine *EGFR* mutation status [1, 9]. A variety of methods, including direct sequencing, PCR-Invader, PNA-LNA PCR clamp, fragment analysis, and Cycleave PCR, were used in the WJTOG3405 phase III study to select *EGFR* mutation-positive patients [2], and the PNA-LNA PCR clamp method was used in the NEJ002 study [3]. To date, a study to compare the sensitivity and concordance of methods for *EGFR* mutation testing in Japan has not been conducted.

Diagnostic practices, and therefore, samples available for *EGFR* mutation analysis, differ between laboratories and countries. Large surgical samples are optimal for *EGFR* mutation analysis but small tissue from a tumor biopsy is the most commonly used and preferred sample type for diagnosis by clinicians [10, 11]. In clinical practice, tissue samples are not always available for diagnosis, and cytology samples, including bronchofiberscopic brushing (BB) cytology and pleural effusion cytology samples, are used in Japan and increasingly globally.

The aim of this study was to evaluate the sensitivity and performance of different *EGFR* mutation tests using artificial DNA admixtures, and clinical samples including formalin-fixed

*Correspondence to: Dr K. Goto, Division of Thoracic Oncology, National Cancer Center Hospital East, Kashiwanoha, 6-5-1, Kashiwa, Chiba, 277-8577, Japan.
Tel: +81-4-7133-1111; Fax: +81-1-7131-4724; E-mail: kgoto@east.ncc.go.jp